CLASP1, astrin and Kif2b form a molecular switch that regulates kinetochore-microtubule dynamics to promote mitotic progression and fidelity.

Amity L Manning*[,1], Samuel F. Bakhoum*[,1], Stefano Maffini[#], Clara C Melo[#], Helder Maiato[#,§], Duane A Compton*

*Department of Biochemistry, Dartmouth Medical School, Hanover, NH 03755; Norris Cotton Cancer Center, Lebanon, NH 03766

[#]IBMC-Instituto de Biologia Molecular e Celular, Universidade de Porto, Rua do Campo Alegre 823, 4150-180 Porto, Portugal

[§]Laboratory of Cell and Molecular Biology, Faculdade de Medicina, Universidade do Porto, 4200-319 Porto, Portugal

[1] Authors contributed equally to this work.

Corresponding Author:

Duane Compton
Dartmouth Medical School
410 Remsen Bldg
Hanover, NH 03766
Office: 603-650-1990
Fax: 603-650-1128
Duane.a.compton@dartmouth.edu

ABSTRACT

Accurate chromosome segregation during mitosis requires precise coordination of various processes such as chromosome alignment, maturation of proper kinetochore-microtubule (kMT) attachments, correction of erroneous attachments, and silencing of the spindle assembly checkpoint (SAC). How these fundamental aspects of mitosis are coordinately and temporally regulated is poorly understood. Here we show that the temporal regulation of kMT attachments by CLASP1, astrin and Kif2b is central to mitotic progression and chromosome segregation fidelity. In early mitosis a Kif2b/CLASP1 complex is recruited to kinetochores where it promotes chromosome movement, kMT turnover, correction of attachment errors, and maintenance of SAC signaling. However, during metaphase, this complex is replaced by an astrin/CLASP1 complex, which promotes kMT stability, chromosome alignment, and silencing of the SAC. We show that these two complexes are differentially recruited to kinetochores and are mutually exclusive. We also show that other kinetochore proteins, such as Kif18a, affect kMT attachments and chromosome movement through these proteins. Thus, CLASP1/astrin/Kif2b act as a central switch at kinetochores that defines mitotic progression and promotes fidelity by temporally regulating kMT attachments.

INTRODUCTION

The most conspicuous events in the cell cycle are the alignment of chromosomes during metaphase and their subsequent segregation in anaphase (Rieder and Khodjakov, 2003). Central to the regulation of these events is the attachment of spindle microtubules to kinetochores. This attachment is highly dynamic as microtubules continuously attach and detach from kinetochores (Zhai et al., 1995). The nature of this dynamic attachment contains several important features. First, kinetochores attach to increasing numbers of microtubules as cells progress through mitosis (McEwen et al., 1997). Second, faithful segregation requires that sister-kinetochores attach to microtubules and bi-orient chromosomes relative to opposite spindle poles (Kapoor and Compton, 2002; Nicklas and Arana, 1992). Third, many kinetochores form erroneous attachments that must be corrected prior to anaphase to ensure accurate chromosome segregation (Salmon et al., 2005). Finally, kinetochores couple chromosome movement to the depolymerization of microtubule plus-ends to generate poleward force for chromosome alignment and segregation (Gorbsky et al., 1987; Kapoor and Compton, 2002), and may also generate antipoleward force (Toso et al., 2009). These aspects of kinetochore-microtubule (kMT) attachments are coordinated such that these associations mature as sister chromatids bi-orient and achieve a tight alignment along the metaphase plate. At the same time, kMT attachments are monitored by the spindle assembly checkpoint (SAC) to ensure that all chromosomes are attached to spindle microtubules before anaphase ensues (Musacchio and Salmon, 2007).

Kinetochores are macromolecular assemblies that mediate the interaction of chromosomes to spindle microtubules and to fulfill this important function, they have

evolved multiple complexes and networks with specific functions (Cheeseman and Desai, 2008; Joglekar et al., 2009; Wan et al., 2009). The KMN (KNL-1/Mis12/NDC80 complex) and Ska1 networks provide core microtubule-binding sites at kinetochores (Cheeseman et al., 2006; Daum et al., 2009; DeLuca et al., 2002; Martin-Lluesma et al., 2002; Welburn et al., 2009). These complexes localize to outer-kinetochores, directly bind microtubules, and *in vitro* assays have shown that they can couple microtubule depolymerization to poleward force (McIntosh et al., 2008; Welburn et al., 2009). Functional perturbation of these components dramatically affects the stability of kMT attachments (DeLuca et al., 2006; DeLuca et al., 2002). Moreover, *in vitro* analyses show that the native affinity of the Ndc80 complex to microtubules is relatively high (Cheeseman et al., 2006). These and other data suggest that these networks provide an *all-or-none* mode of microtubule attachment to kinetochores.

In contrast, direct observation of kMT turnover in unperturbed mitosis in PtK1, LLCPK and human cells reveals much more subtle changes as kMTs mature during mitotic progression. For example, the stability of kMT attachments increases only 2- to 3-fold between prometaphase and metaphase (Bakhoum et al., 2009a; Bakhoum et al., 2009b; Zhai et al., 1995). Furthermore, only slight dampening of kMT attachments is sufficient to severely compromise faithful chromosome segregation, whereas slight destabilization of kMT attachments can reduce the rate of chromosome mis-segregation inherent to human cancer cells that exhibit chromosomal instability (Bakhoum et al., 2009b). Collectively, this reveals the exquisite sensitivity of chromosome segregation fidelity to finely regulated kMT attachment dynamics and points to other components of the outer-kinetochore that would function to *fine-tune* the dynamics of microtubule

attachments downstream of complexes such as the KMN network. However, little is known about the mechanism that provides this fine-tuning, much less the means by which kinetochores coordinate the individual activities of its multiple components to regulate the dynamics of attached microtubules and couple them to error correction mechanisms, force generation, and SAC satisfaction.

Here we use functional and biochemical assays as well as quantitative live-cell fluorescence microscopy coupled with laser-induced photoactivation to explore the mechanisms that underlie the fine-tuning of kMT attachment dynamics. Our work reveals a functional switch at outer-kinetochores that includes CLASP1 (Hannak and Heald, 2006; Maffini et al., 2009; Maiato et al., 2003; Maiato et al., 2005; Maiato et al., 2002; Pereira et al., 2006), astrin (Mack and Compton, 2001; Chang et al., 2001; Gruber et al., 2002; Thien et al., 2007), and the kinesin-13 Kif2b (Manning et al., 2007; Bakhoum et al., 2009b). We also present evidence that other kinetochore-proteins can influence kMT attachment through this group of proteins indicating that they are central regulators of kMT attachments, functionally downstream of other core-binding activities.

RESULTS

Astrin stabilizes microtubules at the outer kinetochore

We sought to identify outer-kinetochore components that play a role in regulating kMT dynamics during mitotic progression. Astrin was identified as an aster-associated protein in mammalian mitotic extracts. It localizes to spindle poles and kinetochores in mammalian cells, yet its kinetochore localization is exclusive to chromosomes that have congressed to the metaphase plate and is absent on those that have not yet congressed (Mack and Compton, 2001; Supplementary Figure 1A). Quantitative immunofluorescence measurements show that total astrin kinetochore localization increased during prometaphase as sister kinetochore pairs progressively achieve biorientation and alignment, such that cells midway through prometaphase (some but not all chromosomes aligned) exhibited 3-fold less astrin kinetochore staining compared to metaphase cells (Supplementary Figure 1B; 0.30 +/- 0.20, $p < 0.00001$, t-test). In addition, astrin co-localized with the Ndc80 complex component Hec1 in human U2OS cells indicating that it is a component of the outer kinetochore (Supplementary Figure 1A), consistent with previous results (Thein et al., 2007).

The temporal localization of astrin to outer-kinetochores is highly unusual and its position at the kinetochore-microtubule interface raises the possibility that it may influence, or be influenced by, kMT attachment dynamics. Indeed, stabilization of kinetochore microtubule attachments with drugs (taxol or stabilizing concentrations of nocodazole) enhanced the localization of astrin to kinetochres and allowed for recruitment of astrin to kinetochores with monotelic and syntelic attachments (Supplementary Figure 1C & D). To test the idea that astrin influences kMT attachment

dynamics, we measured kMT attachment stability in human U2OS cells depleted of astrin using RNA interference. Immunoblot analyses show efficient reduction in astrin following transfection with our siRNA (Supplementary Figure 2A) as well as with the siRNA sequence previously reported by Thein and colleagues (Supplementary Figure 3B). In contrast to that previous report (Thein et al., 007), we did not detect defects in the maintenance of sister chromatid cohesion in astrin-deficient U2OS cells. Mitotic chromosome spreads and centromere staining with CREST sera show that the majority of mitotic cells depleted of astrin using either siRNA sequence maintain sister chromatid cohesion (Supplementary Figure 3; data not shown). Sister chromatid cohesion defects only became apparent following prolonged nocodazole-induced mitotic arrest (20+ hours; Supplementary Figure 3D). Numerous factors influence sister chromatid cohesion including the Retinoblastoma protein (Manning et al., 2010; van Harn et al., 2010). Given that common tissue culture cell lines (including U2OS and HeLa cells) exhibit varying degrees of functional inactivation of the Retinoblastoma protein, among other differences, it is likely that there exists interline variation in how cells maintain chromatid cohesion during mitotic delay in the absence of astrin (Gascoigne and Taylor, 2008). Finally, to discount the possibility of off-target effects of siRNA treatments, we found that siRNA sequences targeting the 3'UTR of the astrin mRNA decrease astrin levels and increase the mitotic index equivalently to siRNA sequences in the coding region used here and the siRNA used by Thein and colleagues (2007). Exogenous expression of GFP-tagged astrin restored the mitotic index to control levels in cells depleted of endogenous astrin following transfection with the 3'UTR siRNA sequence (Supplementary Figure 4).

To directly examine kMT attachment stability, we expressed photoactivatable GFP-tubulin (PA-GFP-tubulin) in human U2OS cells and measured fluorescence dissipation after photoactivation (FDAPA) of spindle microtubules (Figure 1A). The photoactivated region on the spindle decayed at a double exponential decay rate (r^2>0.99), where the slow and fast decaying fluorescence populations corresponded to the stable (kinetochore-associated) and less stable (non-kinetochore associated) microtubule populations, respectively (Bakhoum et al., 2009b; Cimini et al., 2006; Zhai et al., 1995). The half-life of slow-decaying fluorescence is a measure of the average stability of kMT attachments and is inversely proportional to microtubule turnover at the kinetochore (Zhai et al., 1995). kMT stability and half-life are governed by the average rates at which attached microtubules are released from kinetochores. Consistent with astrin enrichment on kinetochores during metaphase in control cells, astrin-deficient U2OS cells show no significant change in kMT stability in prometaphase, but an ~50% decrease in the half-life of kMTs in metaphase (Figure 1C), indicating significantly reduced stability. In addition, kMT stability was not significantly different between control prometaphase cells and astrin-depleted metaphase cells (Figure 1C). This suggests that the temporally delayed recruitment of astrin to kinetochores of congressed chromosomes has a functional relevance towards the maturation of kMT attachment that takes place at the prometaphase-to-metaphase transition. Interestingly, astrin affects kMT dynamics in a manner opposite to that of the kinesin-13 protein, Kif2b, which was shown to destabilize kMT attachments in prometaphase but not in metaphase (Figure 1C, Supplementary Figure 2C; Bakhoum et al., 2009b).

Mutually exclusive complexes of CLASP1/Kif2b and CLASP1/astrin

It was previously shown that GFP-Kif2b also co-localizes with the Ndc80 component Hec1 at outer-kinetochores (Manning et al., 2007). However, this localization is temporally distinct to that of the localization of astrin to kinetochores. The fraction of GFP-Kif2b-positive kinetochores is high in prometaphase and decreases as cells progress to metaphase whereas the fraction of astrin-positive kinetochores increases as cells progress from prometaphase to metaphase (Figure 2A). The low cellular levels of endogenous Kif2b preclude reliable quantitative immunofluorescence, but we have observed endogenous Kif2b localizing to kinetochores and spindle microtubules similar to GFP-Kif2b (Supplementary Figure 5) indicating that GFP-Kif2b is a suitable surrogate for the endogenous protein. Markedly, we have been unable to identify single kinetochores positive for both GFP-Kif2b and astrin, suggesting that their localization is mutually exclusive (Figure 2A). We reasoned that this mutually exclusive localization may be in response to aurora B activity which establishes an activity gradient from the centromere towards sister-kinetochores (Liu et al., 2009). We previously showed that the kinetochore localization of GFP-Kif2b is abolished upon treatment with the aurora inhibitor, hesperadin (Figure 2B; Bakhoum et al., 2009b), indicating that under decreased inter-kinetochore tension in early mitosis aurora kinase activity is required to recruit, directly or indirectly, Kif2b to kinetochores. Strikingly, aurora inhibition had an inverse influence on astrin localization. Hesperadin treatment caused constitutive astrin recruitment to kinetochores, including those that had not achieved bi-oriented attachment, nor had congressed to the metaphase plate (Figure 2B, arrows; Supplementary Figure 1D). This contrasting response to hesperadin treatment unveils a functional mechanism

by which the mutually exclusive recruitment of astrin and Kif2b may occur, where aurora kinase activity oppositely regulates the recruitment of both proteins to kinetochores. This is in agreement with the role of aurora B in temporally regulating kMT turnover by controlling the activities of its kinetochore substrates (Cimini et al., 2006; Liu et al., 2009).

In addition to its dependence on aurora-activity, the kinetochore-localization of GFP-Kif2b relies on a functional Ndc80 complex and the outer kinetochore protein CLASP1 (Manning et al., 2007). Astrin localization to kinetochores was similarly sensitive to these kinetochore constituents, where it was not detectable at kinetochores in Nuf2-deficient mitotic cells (Supplementary Figures 2B and 6B). This dependence of astrin on Nuf2 may reflect a need for stable kinetochore microtubule attachments (Supplementary Figure 1C and D). Moreover, the intensity of astrin at kinetochores was reduced by ~50% in CLASP1-deficient mitotic cells in metaphase (Supplementary Figures 2D and 6A & B). This partial reduction in astrin localization is likely due to the remaining presence of CLASP2 in the CLASP1-depleted cells (Maffini et al., 2009; Mimori-Kiyosue et al., 2006; Pereira et al., 2006) since co-depletion of CLASP1 and CLASP2 decreased astrin kinetochore localization to less than 20% of that seen in control cells (Supplementary Figure 6A & B). Importantly, recent high-resolution-mapping places CLASPs at the outer kinetochore external to the Ndc80 complex (Wan et al., 2009). Together, this shows that despite temporal differences in their kinetochore association, astrin and GFP-Kif2b have shared requirements for Nuf2 and CLASPs in kinetochore localization.

To explore the possibility of a physical interaction between astrin, Kif2b, and

CLASP1, we used astrin and Kif2b-specific antibodies to immunoprecipitate the respective proteins from mitotic cell extracts (Figure 2C). CLASP1 co-precipitated with astrin or Kif2b demonstrating that these proteins form stable complexes at endogenous levels. Markedly, Kif2b did not co-precipitate with astrin and astrin did not co-precipitate with Kif2b (Figure 2C). This suggests that astrin and Kif2b form independent complexes with CLASP1 during mitosis. To further explore this possibility we used GFP-specific antibody for immunoprecipitation from extracts prepared from mitotic cells stably expressing GFP-CLASP1, GFP-astrin, or GFP-Kif2b (Figure 2D). GFP-tagged proteins followed by GFP antibody precipitation were used to overcome protein abundance concerns and because immunoprecipitation with this antibody is highly efficient and provides uniformity for precipitation of different GFP-tagged proteins. GFP-CLASP1 is efficiently precipitated from mitotic extracts with this antibody, and a majority of both astrin and Kif2b co-precipitated with GFP-CLASP1 (Figure 2D, upper left panel). Immunoprecipitation of GFP-astrin co-precipitated a portion of CLASP1 from cells arrested in metaphase (MG132 treated) as expected. However, Kif2b failed to co-precipitate with the GFP-astrin-CLASP1 complex (Figure 2D, upper right panel). Additionally, immunoprecipitation of GFP-Kif2b co-precipitated a portion of CLASP1 but not astrin from prometaphase arrested cells (nocodazole treated) (Figure 2, lower left panel). As a positive control for the selectivity of these immunoprecipitations, we show that LL5-β, a known CLASP1-interacting protein (Lansbergen et al., 2006), was efficiently co-precipitated by the GFP antibody from GFP-CLASP1 expressing cells (Figure 2D, lower right panel). Conversely, specificity of these immunoprecipitations is confirmed by the lack of co-precipitation of alpha-tubulin, and the lack of precipitation of

GFP-CLASP1 with a pre-immune antibody. Although this immunoprecipitation strategy does not directly target the kinetochore-specific populations of these proteins, these data, together with our immunofluorescence observations, strongly suggest that Kif2b and astrin form mutually exclusive complexes with CLASP1 at kinetochores. In addition, treatment of cells with hesperadin, to inhibit Aurora B activity, prior to immunoprecipitation of CLASP1 slightly shifted the preference of CLASP1 for astrin relative to Kif2b (Supplementary Figure 1E). This likely reflects changes in the soluble complexes and suggests that the primary mode of Aurora B regulation is through kinetochore localization of CLASP1/astrin and CLASP1/Kif2b complexes.

We reasoned that these mutually exclusive outer-kinetochore complexes may be used, as a switch, to regulate the temporal changes in kMT stability during the prometaphase-to-metaphase transition. Indeed, both GFP-Kif2b and endogenous Kif2b localization was sensitive to the presence of astrin. In contrast to control cells, where Kif2b only resided at kinetochores in prometaphase, Kif2b persisted on many bi-oriented kinetochores during metaphase in astrin-deficient cells (Figure 3; Supplementary Figure 5). Specifically, GFP-Kif2b primarily localized to only one of two bi-oriented sister-kinetochores in astrin-deficient cells. This result suggests that increased kMT turnover in astrin-deficient cells in metaphase could be due to the constitutive localization of Kif2b/CLASP1 complex at kinetochores. To test this idea, we measured kMT dynamics in cells depleted of both astrin and Kif2b. The effect of depleting both astrin and Kif2b on kMT stability in prometaphase was not significantly different from the effect of depleting Kif2b alone (Figure 1C; Bakhoum et al., 2009b), befitting the absence of astrin from kinetochores during this phase of mitosis. However, simultaneous depletion of

Kif2b and astrin restored kMT attachment stability to control levels in metaphase and led to a significant increase in attachment stability compared to cells lacking astrin alone (Figure 1C). This shows that the astrin/CLASP1 complex may not have an intrinsic role in stabilizing kMT attachments, but that this complex suppresses microtubule turnover at kinetochores by limiting the activity of Kif2b/CLASP1 in a temporal fashion to allow for the maturation of kMT attachments.

Force generation at kinetochores is regulated by CLASP1/astrin/ Kif2b

In addition to regulating the rates of microtubule attachment and detachment, kinetochores harness the energy from depolymerizing microtubules to produce poleward force for chromosome movement. We previously showed that the velocity of chromosome movement in prometaphase is significantly reduced in Kif2b-deficient U2OS cells (Manning et al., 2007). This suggests that Kif2b/CLASP1 may participate in the conversion of microtubule depolymerization into poleward force at kinetochores, and we tested this idea using a functional assay previously developed to detect force generation at kinetochores by examining their effect on spindle pole organization (Figure 4A; Manning and Compton, 2007). In this assay, inhibition of the microtubule cross-linkers and pole-organizing proteins, NuMA and HSET, renders spindle poles sensitive to poleward forces generated at kinetochores, resulting in splaying of spindle poles. This can be rescued by abolishing forces at kinetochores either by inhibiting kMT attachments or, in principle, by abolishing this poleward force despite the presence of kinetochore-fibers (Figure 4A). Injection of inhibitory antibodies specific to the pole focusing proteins NuMA and HSET led to splaying of spindle poles in >99% of U2OS cells

(Figure 4B, n = 150 cells). However, pole focusing, in the absence of the functions of NuMA and HSET, was preserved in these cells if force production at kinetochores was abolished by disrupting kMT attachments via the depletion of the Ndc80 complex constituent Nuf2 (Figure 4B; Manning and Compton, 2007). In this case, 92% of Nuf2-deficient injected cells exhibited focused spindle poles (Figure 4B, n = 99 cells). We reasoned that if Kif2b/CLASP1 participates in force generation at kinetochores, then its depletion should restore pole focusing in this functional assay despite of the presence of kMT attachments. The localization of GFP-Kif2b at kinetochores depends on the Ndc80 complex, however depletion of Kif2b does not perturb Nuf2 levels at kinetochores (Manning et al., 2007). Strikingly, 70% of Kif2b-deficient injected cells displayed spindles with focused poles (Figure 4B, n = 70 cells). Similarly, the majority of CLASP1-deficient injected cells (55%) also display focused spindle poles albeit to a somewhat lesser extent, but not significantly different than Kif2b (Figure 4B, n = 70 cells). Only a minority of astrin-deficient injected cells form spindles with focused poles, confirming the specificity of this assay (34%, n = 57 cells). These data indicate that the Kif2b/CLASP1 complex acts downstream of Nuf2 to generate sufficient force in early mitosis to promote chromosome movement (Manning et al., 2007).

CLASP1/astrin/ Kif2b modulate chromosome oscillation

Next, we examined the role of astrin and Kif2b in the characteristic oscillations of chromosomes by testing its functional relationship to Kif18a, a kinesin-8 that plays an important role in promoting chromosome congression by suppressing the amplitude of oscillatory movement of chromosomes (Stumpff et al., 2008). Kif18a depletion

abolished the localization of astrin to kinetochores (Figure 5A) despite the establishment of bi-oriented kMT attachments shown previously (Mayr et al., 2007). Accordingly, GFP-Kif2b persisted on single kinetochores of bi-oriented chromosomes (Figure 5A). Kif18a localization was not detectably changed in astrin- or Kif2b-deficient cells (Supplementary Figure 7) suggesting that Kif18A acts functionally upstream of these proteins.

To follow chromosome oscillations at high resolution, we used live cell imaging to track kinetochore pairs in U2OS cells expressing CenpB-GFP (Figure 6A). We measured the deviation from the average position (DAP) of individual kinetochores, which is indicative of the amplitude of oscillation (Figure 6B & C; Stumpff et al., 2008). In untreated control cells, sister-kinetochores oscillated with an average DAP of 0.4μm (Figure 6B & C). Depletion of Kif2b led to slight dampening in chromosome oscillation, nevertheless, chromosomes eventually congressed to the metaphase plate and kinetochores displayed reduced DAP levels. This is similar to the inhibition of CLASP1 using antibody injection (Maiato et al., 2003). As previously reported, depletion of Kif18a led to hyper-oscillation of sister-kinetochores, significant increase in DAP values, and abrogation of chromosome alignment (Stumpff et al., 2008). Strikingly, simultaneous depletion of Kif18A and Kif2b virtually abolished chromosome movement (Figure 6A-C). Accordingly, DAP values in these cells were near-zero (Figure 6C). To verify that the lack of chromosome movement in these cells was not due to complete disruption of kMT attachments, we treated mitotic cells that were simultaneously depleted of Kif2b and Kif18A with $CaCl_2$ and found that they possessed Ca^{2+}-stable microtubules (Supplementary Figure 8), indicating they established bioriented kMT

attachments. Moreover, these cells had typical overall inter-kinetochore distances (Figure 6C) showing that they established bioriented kMT attachments. However, the distance between sister-kinetochores did not significantly fluctuate over time (Figure 6C), a likely consequence of the near-complete abrogation of kinetochore movement. Comparing the magnitude of fluctuation of inter-kinetochore distances in Kif18a, Kif2b, and Kif18a/Kif2b-depleted cells suggests that Kif18a functions to coordinate sister-kinetochore movements during chromosome oscillation. Together, these data suggest that deregulation of Kif2b underlies the hyper-oscillation of chromosomes observed in Kif18A-deficient cells and that Kif18a modulates kMT dynamics in part by favoring the kinetochore-recruitment of the astrin/CLASP1 complex, which, in turn, curtails the constitutive activity of the Kif2b/CLASP1 complex at kinetochores. This fits with studies of kinetochore oscillation showing that metaphase plates become tighter just before cells enter anaphase (Jaqaman et al., 2010). It is important to note that the deregulation of Kif2b by itself is not sufficient to produce kinetochore hyper-oscillation. In astrin-depleted cells, GFP-Kif2b persists on bi-oriented kinetochores yet chromosomes efficiently align in these cells and there is no evidence of increased oscillation. Thus, it is the combined effect of Kif18a absence and constitutive localization of Kif2b that leads to kinetochore hyper-oscillation, suggesting that Kif18a utilizes its motor activity to directly suppress kinetochore oscillation and oppose Kif2b activity.

The persistent localization of Kif2b/CLASP1 to kinetochores in Kif18a-deficient cells predicts that kMT attachment stability should be reduced relative to those in control cells. Therefore, we tested kMT stability in Kif18a-deficient cells and found that they displayed significantly less stable kMT attachments compared to control cells at

metaphase (Figure 5B), although the lack of tight chromosome alignment in Kif18a-deficient cells makes it impossible to accurately define these mitotic cells as prometaphase or metaphase. The simultaneous depletion of Kif18a and Kif2b significantly increased kMT attachment stability, akin to the depletion of Kif2b or CLASP1 alone (Figure 5B; Maffini et al., 2009). Furthermore, Kif18a-deficient cells failed to preserve focused spindle poles upon inhibition of NuMA and HSET (Figure 4B) as < 7% of cells exhibited focused poles (n = 30), supporting the idea that kinetochores exhibit poleward force sufficient to splay spindle poles in the absence of Kif18a and that this force may be responsible for kinetochore hyper-oscillation in the absence of Kif18a. Thus, Kif18a modulates the activity of Kif2b and astrin to couple chromosome alignment with the maturation of kinetochore fibers leading to the establishment of metaphase.

Mitotic consequences of deregulated kMT attachments

The progressive stabilization of kMT attachments during the transition from prometaphase to metaphase contributes to silencing of the spindle assembly checkpoint (SAC) and preservation of appropriately oriented kMT attachments necessary for faithful chromosome segregation (Cimini et al., 2003; McEwen et al., 2001; McEwen and Dong, 2009; McEwen et al., 1997; Musacchio and Hardwick, 2002). Depletion of astrin or Kif18a reduced kMT attachment stability by ~2-fold (Figure 1B and 5B). This triggered a SAC-mediated mitotic arrest, as judged by an increase in the mitotic index and the presence of mad2 on some aligned kinetochores (Figure 7A & B). Depletion of Kif2b also increased the mitotic index (Figure 7A), but this was due to the formation of transient monopolar spindles that subsequently resolve into bipolar spindles and then

proceed into anaphase in a timely manner (Bakhoum et al., 2009b). Interestingly, both the mitotic arrest and mad2-localization on aligned kinetochores in Kif18a- or astrin-deficient cells were relieved (Figure 7A & B) when kMT stability was restored by the simultaneous depletion of Kif2b (Figure 1C and 5B; co-depletion also rescued the transient monopolar spindle phenotype observed upon the depletion of Kif2b alone). This indicates that the constitutive localization of Kif2b at kinetochores in cells lacking either astrin or Kif18a destabilizes kMT attachments which delays silencing of the SAC. This is also consistent with previous observations showing that cells do not tolerate excessive levels of GFP-Kif2b and provides a strong account for the low endogenous levels of Kif2b (Bakhoum et al., 2009b; Manning et al., 2007). To independently test the relationship between kMT stability and silencing of the SAC, Kif18a- or astrin-deficient cells were also depleted of a second microtubule-destabilizing kinesin-13 protein, MCAK (Bakhoum et al., 2009b). MCAK depletion does not affect spindle geometry in U2OS cells (Bakhoum et al., 2009b) and its co-depletion with either astrin or Kif18a restored kMT stability (data not shown) and silenced the SAC (Figure 7A).

On the other hand, hyperstable kMT attachments prevent correction of maloriented microtubules and increase the rate of chromosome mis-segregation (Bakhoum et al., 2009b; Cimini et al., 2006; DeLuca et al., 2006). Accordingly, manipulations of these proteins that stabilized kMT attachments beyond control levels led to a proportional increase in the incidence of chromosome segregation errors as judged by elevated frequencies of lagging chromosomes (Figure 7C & D and Supplementary Figure 9). For example, depletion of Kif2b stabilizes kMT attachments resulting in an increase in the presence of lagging chromosomes during anaphase. This effect is specific

to the loss of Kif2b because depletion of endogenous Kif2b using an siRNA sequence derived from the 5'UTR yields a similar increase in the frequency of lagging chromosomes and this is rescued by the expression of GFP-Kif2b which is not targeted by the 5'UTR siRNA (Supplementary Figure 9). In addition, kMT attachments were stabilized in prometaphase by the simultaneous depletion of Kif2b and astrin (Figure 1C), and those cells displayed increased frequencies of lagging chromosomes at anaphase (Figure 7C). kMTs were also excessively stable in cells simultaneously depleted of Kif18a and Kif2b (Figure 5B) or MCAK (data not shown) and those cells displayed elevated frequencies of lagging chromosomes relative to control cells (Figure 7C). Thus, the molecular switch between Kif2b/CLASP1 and astrin/CLASP1 generates appropriate kMT attachment dynamics to promote the correction of kMT attachment errors and preserve genome stability. Importantly, these data indicate that these proteins ensure that kMT attachments fall within a permissible range required for error-free mitotic progression.

DISCUSSION

This work defines a molecular switch at the outer kinetochore, whereby an astrin/CLASP1 complex replaces a Kif2b/CLASP1 complex as chromosomes form bioriented spindle attachments during the transition from prometaphase to metaphase. This switch is central to coordinating various events during mitosis including the maturation of kMT attachments, silencing of the SAC, chromosome movement and alignment, and correction of attachment errors.

Historically, chromosome alignment at the metaphase plate was the sole criteria used to define this transition (Rieder and Khodjakov, 2003). This morphologic definition left the molecular underpinnings of the transition from prometaphase to metaphase unknown and here we provide a molecular definition of this stage of mitotic progression. Kif2b/CLASP1 localizes to kinetochores in early mitosis where it utilizes its microtubule depolymerizing activity to promote kMT dynamics typical of prometaphase cells. This activity prevents kinetochore saturation with microtubules, thereby maintaining SAC signaling (McEwen et al., 1997), and enabling the correction of attachment errors that frequently occur in this phase of mitosis due to stochastic interactions of microtubules with kinetochores (Bakhoum et al., 2009b; Cimini et al., 2003). Furthermore, it also enables poleward movement of chromosomes on microtubules that is characteristic of chromosome oscillation during prometaphase. The recruitment of astrin/CLASP1 upon bi-orientation of sister-kinetochores in place of the Kif2b/CLASP1 complex results in the stabilization of kMTs, thereby promoting silencing of the SAC. Kinetochores in astrin-deficient U2OS cells form bi-oriented attachments and chromosomes align at the spindle equator. However, these cells do not proceed into anaphase in a timely manner indicating

that despite chromosome alignment, a functional metaphase state is not achieved. A similar effect has also been observed upon perturbation of the Ska complex (Daum et al., 2009; Welburn et al., 2009). Conversely, the mitotic index of cells lacking both Kif18a and Kif2b is low indicating that they satisfy the SAC and enter anaphase in a timely fashion, yet they do so with kinetochores that fail to exhibit normal oscillation and alignment. Thus, metaphase and the onset of anaphase are primarily dependent on the maturation of kinetochore-fibers induced by molecular changes at kinetochores rather than the physical position and motion of chromosomes along the mitotic spindle (Rieder et al., 1995). Furthermore, our data suggests that chromosome oscillation is not required for the onset of anaphase.

At the outer kinetochore, CLASPs play key roles in linking dynamic microtubules to chromosomes (Hannak and Heald, 2006; Maffini et al., 2009; Maiato et al., 2003; Maiato et al., 2005; Maiato et al., 2002; Pereira et al., 2006). Our data indicate that CLASPs fulfill that role, in part, by recruiting different proteins to the outer kinetochore. Because CLASP1 physically associates with Kif2b and astrin, yet recruits these proteins to the outer kinetochore at different stages of mitosis, we propose that it provides a scaffolding activity to temporally regulate the targeting of different proteins to outer kinetochores. CLASPs levels at kinetochores decrease from prometaphase to metaphase (Maiato et al., 2003; Pereira et al., 2006) and the rapid cycling of CLASPs between kinetochore-bound and soluble pools (Pereira et al., 2006) provides the opportunity for the replacement of the Kif2b-CLASP1 complex in early prometaphase with the astrin-CLASP1 complex in late prometaphase and through anaphase. The very low abundance of Kif2b (Manning et al., 2007) relative to astrin makes models invoking competitive

binding of either Kif2b or astrin to CLASP1 unlikely. Instead, our data implicates aurora kinase activity in regulating the replacement of Kif2b/CLASP1 with astrin/CLASP1 at outer kinetochores, in a manner similar to its regulation of the KMN network (Cheeseman et al., 2006; DeLuca et al., 2006). In prometaphase, inter-kinetochore distance is sufficiently low to allow the aurora B activity gradient to reach its outer kinetochore substrates (Liu et al., 2009). This activity recruits the Kif2b/CLASP1 complex (Bakhoum et al., 2009b; E. Logarinho and H. Maiato, unpublished observations). As kinetochores establish bi-oriented attachments, they become further separated, displacing aurora B activity from its kinetochore substrates (Liu et al., 2009). This leads to the recruitment of the astrin/CLASP1 complex to kinetochores to replace the Kif2b/CLASP1 complex (Figure 7E).

A key feature of this molecular switch at outer kinetochores is that it *fine tunes* kMT attachments to ensure that their stability falls within a permissible range that allows the simultaneous satisfaction of the SAC and faithful chromosome segregation. Perpetually reduced kMT attachment stability delays the silencing of the SAC whereas hyperstable attachments compromise the correction of attachment errors (which require the release of erroneously attached microtubules from kinetochores) and lead to chromosome mis-segregation. Importantly, perturbation of components of this molecular switch reveals the exquisite sensitivity of error-free mitotic progression to minor perturbation of kMT attachment stability. The permissible range of kMT stability is relatively narrow, where the half-life of kMTs must fall within the order of a few minutes to satisfy accurate mitotic requirements. The 2- to 3-fold increase in kMT attachment stability during the prometaphase-to-metaphase transition does not appear to be achieved

by the Ndc80 complex, which acts as an all-or-none switch and affects kMT dynamics by ~10-100-fold. Therefore, this molecular switch provides an additional and essential layer of precision to regulate kMT attachments ancillary to the core binding properties provided by the Ndc80 complex.

Identification of these regulators of kMT dynamics provides insight into the mechanisms that couple microtubule depolymerization to force generation at kinetochores during mitosis. *In vitro* experiments have demonstrated that microtubule depolymerization is sufficient to power chromosome movement (Coue et al., 1991; Grishchuk et al., 2005; Koshland et al., 1988). In principle, chromosome movement could be driven by spontaneous microtubule depolymerization if the depolymerizing microtubules were processively attached to Ndc80 or Ska1 complexes (Cheeseman et al., 2006; Daum et al., 2009; Welburn et al., 2009). However, poleward chromosome movement is significantly reduced in prometaphase by inhibition of the Kif2b/CLASPs complex despite the presence of the Ndc80 complex and calcium-stable kMT attachments (Manning et al., 2007). This demonstrates the requirement for microtubule-depolymerizing factors at outer kinetochores to regulate the dynamics of microtubules and enhance their depolymerization rates in vivo. It remains unknown if the processive action of these microtubule depolymerases is required for continual force generation, or if their catalytic function is limited to simply triggering the depolymerization of kMTs. In contrast, once chromosomes achieve bi-oriented kMT attachments, Kif2b/CLASP1 is displaced by astrin/CLASP1 and thus force for chromosome alignment and segregation must come from other sources such as dynein, CenpE, the NAC/CAD complex or Kif18a (Howell et al., 2001; Kapoor et al., 2006; Amaro et al., 2010; Stumpff et al., 2008).

Thus, this data shows that the responsibility for generating poleward force for chromosome movement shifts as cells transit from one stage of mitosis to another. Specifically, we show that the Kif2b/CLASP1 kinetochore complex is responsible for generating poleward force at kinetochores in early mitosis and that its function is replaced by Kif18a which produces balanced and opposed forces on sister-kinetochores to align mitotic chromosomes, making it a likely candidate for force-generation during metaphase.

In summary, we show that central to events that take place during mitotic progression is the precise and timely regulation of kMT attachments. We have shown that this is achieved by the temporal recruitment of mutually exclusive protein complexes to kinetochores. Given the complex nature of the outer-kinetochore it is likely that other protein components, such as the recently identified astrin-binding protein SKAP (Jens Schmidt and Iain Cheeseman; personal communication), play essential roles in this regulation through the proteins examined here.

MATERIALS AND METHODS

Cell Culture

Human U2OS and HeLa cells were maintained in Dulbecco's modified medium containing 10% FBS, 50 IU/ml penicillin, and 50 μg/ml streptomycin.

Antibodies

Antibodies used in this work included HSET (Mountain et al., 1999), Kif2a (Ganem and Compton, 2004), NuMA (Gaglio et al., 1995), DM1α (Sigma-Aldrich), Hec1 (Novus Biologicals), actin-specific monoclonal antibody (provided by Harry Higgs, Dartmouth Medical School, Hanover, NH), Mad2, Kif2b (Manning et al., 2007), astrin (Mack and Compton, 2001), ZW10 (Gift from Conly Rieder, Wadsworth Center, New York), GFP, LL5β (Gift from Anna Akhmanova, Erasmus University, Rotterdam, The Netherlands), and CLASP1 Rb2292 (Gift from Niels Galjart, Erasmus University, Rotterdam, The Netherlands).

RNA Interference

Nuf2, Kif2a, astrin, Kif18A, ZW10, CLASP1, CLASP2, Sgo1, MCAK, and Kif2b levels were reduced using published sequences (DeLuca et al., 2002; Ganem and Compton, 2004; Manning et al., 2007; Stumpff et al., 2008; Thein et al., 2007; Yang et al., 2007). The sequence of the sense strand of siRNA duplexes targeting the 5' UTR of Kif2b was 5'-UGAUACCUCCAUCACUCAC-3', the coding region of astrin was 5'-GGCCCGUUUAGAUACCAUG-3', and the 3' UTR of astrin was 5'-CCAACUGAGAUAAAUGCU-3' and 5'-CAAUACCAAGACCAACUGG-3', each

synthesized with 3' dTdT overhangs. Approximately 30,000 U2OS cells were plated on coverslips in 35-mm dishes the day before transfection and grown without antibiotics. Double stranded RNAs were transfected into cells using Oligofectamine^{TM} reagent (Invitrogen) as described previously (Manning and Compton, 2007). To ensure optimal knockdown of target, cells were transfected with double strand RNAs twice, with the second transfection occurring 24 hours after the first. Cells were microinjected 48h after first transfection and analyzed 72h after first transfection by indirect immunofluorescence or immunoblot analysis.

Immunoblotting

For immunoblots, cultured cells were solubilized directly in 1X SDS-PAGE sample buffer. Total cell protein was then separated by size using SDS-PAGE and transferred to PVDF membrane (Millipore Corp.). Primary antibodies were incubated for 1 hr. at room temperature in 1% milk Tris-buffered saline (TBS). Primary antibody was then detected using HRP-conjugated secondary antibodies (Bio-Rad Co.) diluted in TBS for an additional 1 h. at room temperature. The signal was then detected using chemiluminescence.

GFP-Tubulin photoactivation

As previously described (Bakhoum et al., 2009b; Cimini et al., 2006; Zhai and Borisy, 1994), mitotic cells were identified by D.I.C. microscopy and several pulses from a 405 nm diffraction-limited laser (Photonic Instruments, St Charles, IL) were used to photoactivate and area of $< 2\ \mu m^2$ of GFP within the spindle as previously described.

Images were acquired with a Hamamatsu Orca II camera binned 2 X 2 with a 63X, 1.4 NA objective on a Zeiss Axioplan 2 microscope. 3 x 1-μm stacks of fluorescent images were collected <1s before and after photoactivation. Subsequently, images were collected every 30 s. D.I.C. microscopy was then used to verify that cells did not undergo anaphase.

Photoactivation analysis

FDAPA analysis was performed primarily as described previously (Bakhoum et al., 2009b; Cimini et al., 2006; Zhai and Borisy, 1994). Briefly, pixel intensities were measured within a ~2 μm^2 rectangular area surrounding the region with the brightest fluorescence and pixel intensities from an equal area from the opposite half-spindle were subtracted. Correction for photobleaching was made by normalizing to values obtained from photoactivated taxol-stabilized spindles where the photoactivatable region clearly did not dissipate. Bleaching-induced decrease in average fluorescence after 30-captured images was 35%. For each cell, fluorescence values were normalized to the first time-point after photoactivation. Normalized fluorescence was then averaged for multiple cells at each time-point. A double exponential regression analysis was used to fit the data to the following equation: $F(t) = A_1 e^{-k_1 t} + A_2 e^{-k_2 t}$, where $F(t)$ is measured photoactivated fluorescence at time t, A_1 and A_2 represent less (non-kinetochore-associated) and more (kinetochore-associated) stable microtubule populations with decay rate constants of k_1 and k_2, respectively.

Microinjection, DIC, Phase and Indirect immunofluorescence microscopy

Antibody preparation and microinjcetion were performed as previously described (Manning and Compton, 2007). The following antibody concentrations refer to antibody concentrations in the microinjection needle: 20 mg/ml α-NuMA, 10mg/ml α-NuMA/15 mg/ml α-HSET (mixed), and 19 mg/ml nonimmune IgG. Cells were followed by phase microscopy until they entered mitosis at which point they were processed for immunofluorescence imaging.

For indirect immunofluorescence, U2OS cells were extracted in microtubule-stabilizing buffer (4 M glycerol, 100 mM Pipes, pH 6.9, 1 mM EGTA, 5 mM MgCl2, and 0.5% Triton X-100), followed by fixation in 1% glutaraldehyde. For endogenous Kif2b staining, cells were prepared and fixed according to Maiato et al., 2003. Subsequent antibody incubations and washes were done in TBS-BSA (10 mM Tris, pH 7.5, 150 mM NaCl, and 1% BSA). Primary antibodies were detected using species–specific fluorescein- Cy5-, or Texas red–conjugated secondary antibodies (Vector Laboratories). DNA was detected with 0.2 μg/ml DAPI (Sigma-Aldrich). Coverslips were mounted with ProLong Antifade mounting medium (Molecular Probes). Fluorescent images of fixed cells were captured with a Hammamatsu Orca ER cooled CCD camera mounted on an Eclipse TE 1000-E Nikon microscope with a 60X 1.4 n.a. objective. A series of 0.25 μm optical sections were collected in the z plane for each channel (DAPI, fluorescein, Cy5 and/or Texas red). Iterative Restoration was performed on images using Phylum software (Improvision Inc). Selected planes from the z-series were then overlaid to generate the final image. Cells were treated with the Eg5 inhibitor monastrol (100μM), and/or MG132 (5μM) and Hesperadin (50nM), or microtubule stabilizing concentrations of taxol (100nM) or nocodazole (100nM) prior to fixation and staining for astrin and

GFP-Kif2b imaging. For comparative measurements of average pixel intensity for astrin staining, kinetochores were identified and selected based on Hec1 staining. Measurements were normalized to measured average pixel intensities of astrin kinetochore staining in metaphase cells from the same experiment.

Immunoprecipitation

Immunoprecipitation experiments were performed with aliquots of native protein extracts (3 mgs of total protein in a total volume of 500 µl of IP buffer: 150mM KCl, 75mM Hepes p.H 7.5, 1.5 mM EGTA, 1.5 mM $MgCl_2$, 10 % glycerol, 0.1 % NP40, protease inhibitors) prepared from untreated HeLa cells, HeLa cells stably expressing either EGFP-CLASP1 (Pereira et al., 2006) or EGFP-astrin, untreated U2OS cells or U2OS cells stably expressing EGFP-Kif2b. Mitotic cells were enriched by incubation with 3 µM nocodazole for 16 hours. Following nocodazole arrest, EGFP-astrin cells were washed and then released, for 1 hour, in media containing MG132 (5µM). Alternatively, following nocodazole arrest, EGFP-CLASP1 cells were washed and released for 40 minutes into media containing MG132 (5µM) or MG132 and Hesperadin (50nM). Protein extracts were incubated with the precipitating antibody at 4^{o}C for 4 hours on a rotating platform. Precipitating primary antibodies used were rabbit anti-GFP and rabbit anti-GFP pre-immunization serum (GFP-PI) or rabbit astrin and rabbit Kif2b serum. These extracts were then incubated with 40 µl of protein A-Sepharose slurry for 2 hours at 4^{o}C on a rotating platform. Samples were centrifuged, the supernatant was retained as unbound sample and the pelleted beads washed 5 times with washing buffer (IP buffer with 250mM KCl). Precipitated proteins were removed from the beads by boiling 5

minutes in SDS sample buffer and subjected to electrophoresis on a 7.5% gel, followed by western blot analysis with the appropriate antibody (anti-GFP, 1:1000; anti-Astrin, 1:1000; anti-Kif2b, 1:1000 ; anti-LL5β, 1:2000; anti-α-tubulin, 1:5000, clone B-12, Sigma-Aldrich; anti-CLASP1 Rb2292, 1:1000).

ACKNOWLEDGEMENTS

We would like to thank Niels Galjart, Anna Akhmanova (Erasmus Medical Center, Rotterdam, The Netherlands), and Conly Rieder (Wadsworth Center, NewYork, USA) for the kind gift of antibodies. S.M. holds a post-doctoral fellowship (SFRH/BPD/34905/2007) from Fundação para a Ciência e a Tecnologia (FCT) of Portugal. A.L.M. is supported by a John H. Copenhaver, Jr. and William H. Thomas, M.D. 1952 Junior Fellowship. Work in the lab. of H.M. is supported by grants PTDC/BIA-BCM/66106/2006, PTDC/SAU-OBD/66113/2006 and PTDC/SAU-GMG/099704/2008 from FCT (FEDER), and the European Research Council grant PRECISE. Work in the lab of D.A.C. is supported by National Institutes of Health grant GM51542. The authors declare that they have no conflict of interest.

REFERENCES

Amaro AC, Samora CP, Holtackers R, Wang E, Kingston IJ, Alonso M, Lampson M, McAinsh AD, Meraldi P (2010) Molecular control of kinetochore-microtubule dynamics controls chromosome oscillations. *Nature Cell Biol* **12**:319-329.

Bakhoum SF, Genovese G, and Compton DA (2009a) Deviant Kinetochore Microtubule Dynamics Underlie Chromosomal Instability. *Curr Biol* **19**:1937-1942.

Bakhoum SF, Thompson SL, Manning AL, and Compton DA (2009b) Genome stability is ensured by temporal control of kinetochore-microtubule dynamics. *Nature Cell Biol* **11**:27-35.

Chang MS, Huang CJ, Chen ML, Chen ST, Fan CC, Chu JM, Lin WC, and Yang YC (2001) Cloning and characterization of hMAP126, a new member of mitotic spindle-associated proteins. *Biochem Biophys Res Commun* **287**:116-121.

Cheeseman IM, Chappie JS, Wilson-Kubalek EM, and Desai A (2006) The conserved KMN network constitutes the core microtubule-binding site of the kinetochore. *Cell* ***127***:983-997.

Cheeseman IM, and Desai A (2008) Molecular architecture of the kinetochore-microtubule interface. *Nature Rev Mol Cell Biol* **9**:33-46.

Cimini D, Moree B, Canman JC, and Salmon ED (2003) Merotelic kinetochore orientation occurs frequently during early mitosis in mammalian tissue cells and error correction is achieved by two different mechanisms. *J Cell Sci* **116**:4213-4225.

Cimini D, Wan XH, Hirel CB, and Salmon ED (2006) Aurora kinase promotes turnover of kinetochore microtubules to reduce chromosome segregation errors. *Curr Biol* **16**:1711-1718.

Coue M, Lombillo VA, and Mcintosh JR (1991) Microtubule Depolymerization Promotes Particle and Chromosome Movement Invitro. *J Cell Biol* **112**:1165-1175.

Daum JR, Wren JD, Daniel JJ, Sivakumar S, McAvoy JN, Potapova TA, and Gorbsky GJ (2009) Ska3 Is Required for Spindle Checkpoint Silencing and the Maintenance of Chromosome Cohesion in Mitosis. *Curr Biol* **19**:1467-1472.

DeLuca JG, Gall WE, Ciferri C, Cimini D, Musacchio A, and Salmon ED (2006) Kinetochore microtubule dynamics and attachment stability are regulated by Hec1. *Cell* **127**:969-982.

DeLuca JG, Moree B, Hickey JM, Kilmartin JV, and Salmon ED (2002) hNuf2 inhibition blocks stable kinetochore-microtubule attachment and induces mitotic cell death in HeLa cells. *J Cell Biol* **159**:549-555.

Gaglio T, Saredi A, and Compton DA (1995) NuMA is required for the organization of microtubules into aster-like mitotic arrays. *J Cell Biol* **131**:693-708.

Ganem NJ, and Compton DA (2004) The KinI kinesin Kif2a is required for bipolar spindle assembly through a functional relationship with MCAK. *J Cell Biol* **166**:473-478.

Gascoigne KE, and Taylor SS (2008) Cancer cells display intra- and interline variation profound following prolonged exposure to antimitotic drugs. *Cancer Cell* **14**:111-122.

Gorbsky GJ, Sammak PJ, and Borisy GG (1987) Chromosomes move poleward in anaphase along stationary microtubules that coordinately disassemble from their kinetochore ends. *J Cell Biol* **104**:9-18.

Grishchuk EL, Molodtsov MI, Ataullakhanov FI, and McIntosh JR (2005) Force production by disassembling microtubules. *Nature* **438**:384-388.

Gruber J, Harborth J, Schnabel J, Weber K, and Hatzfeld M (2002) The mitotic-spindle-associated protein astrin is essential for progression through mitosis. *J Cell Sci* **115**:4053-4059.

Hannak E, and Heald R (2006) Xorbit/CLASP links dynamic microtubules to chromosomes in the Xenopus meiotic spindle. *J Cell Biol* **172**:19-25.

van Harn R, Foijer F, van Vugt M, Banerjee R, Yang F, Oostra A, Joenje H, and te Riele H (2010) Loss of Rb proteins causes genomic instability in the absence of mitogenic signaling. *Genes Dev* **24**:1377-1388.

Howell BJ, McEwen BE, Canman JC, Hoffman DB, Farrar EM, Rieder CL, and Salmon ED (2001) Cytoplasmic dynein/dynactin drives kinetochore protein transport to the spindle poles and has a role in mitotic spindle checkpoint inactivation. *J Cell Biol* **155**:1159-1172.

Jaqaman K, King EM, Amaro AC, Winter JR, Dorn JF, Elliott HL, Mchedlishvili N, McClelland SE, Porter IM, Posch M, Toso A, Danuser G, McAinsh AD, Meraldi P, and Swedlow JR (2010) Kinetochore alignment within the metaphase plate is regulated by centromere stiffness and microtubule depolymerases. *J Cell Biol* **188**:665-679.

Joglekar AP, Bloom K, and Salmon ED (2009) In Vivo Protein Architecture of the Eukaryotic Kinetochore with Nanometer Scale Accuracy. *Curr Biol* **19**:694-699.

Kapoor TM, and Compton DA (2002) Searching for the middle ground: mechanisms of chromosome alignment during mitosis. *J Cell Biol* **157**:551-556.

Kapoor TM, Lampson MA, Hergert P, Cameron L, Cimini D, Salmon ED, McEwen BF, and Khodjakov A (2006) Chromosomes can congress to the metaphase plate before biorientation. *Science* **311**:388-391.

Koshland DE, Mitchison TJ, and Kirschner MW (1988) Polewards Chromosome Movement Driven by Microtubule Depolymerization In vitro. *Nature* **331**:499-504.

Liu D, Vader G, Vromans MJM, Lampson MA, and Lens SMA (2009) Sensing Chromosome Bi-Orientation by Spatial Separation of Aurora B Kinase from Kinetochore Substrates. *Science* **323**:1350-1353.

Mack GJ, and Compton DA (2001) Analysis of mitotic microtubule-associated proteins using mass spectrometry identifies astrin, a spindle-associated protein. *Proc Natl Acad Sci, USA* **98**:14434-14439.

Maffini S, Maia ARR, Manning AL, Maliga Z, Pereira AL, Junqueir M, Shevchenko A, Hyman A, Yates JR, Galjart N, Compton DA, and Maiato H (2009) Motor-Independent Targeting of CLASPs to Kinetochores by CENP-E Promotes Microtubule Turnover and Poleward Flux. *Curr Biol* **19**:1566-1572.

Maiato H, Fairley EAL, Rieder CL, Swedlow JR, Sunkel CE, and Earnshaw WC (2003) Human CLASP1 is an outer kinetochore component that regulates spindle microtubule dynamics. *Cell* **113**:891-904.

Maiato H, Khodjakov A, and Rieder CL (2005) Drosophila CLASP is required for the incorporation of microtubule subunits into fluxing kinetochore fibres. *Nature Cell Biol* **7**:42-47.

Maiato H, Sampaio P, Lemos CL, Findlay J, Carmena M, Earnshaw WG, and Sunkel CE (2002) MAST/orbit has a role in microtubule-kinetochore attachment and is essential for chromosome alignment and maintenance of spindle bipolarity. *J Cell Biol* **157**:749-760.

Manning AL, and Compton DA (2007) Mechanisms of spindle-pole organization are influenced by kinetochore activity in mammalian cells. *Curr Biol* **17**:260-265.

Manning AL, Ganem NJ, Bakhoum SF, Wagenbach M, Wordeman L, and Compton DA (2007) The kinesin-13 proteins Kif2a, Kif2b, and Kif2c/MCAK have distinct roles during mitosis in human cells. *Mol Biol Cell* **18**:2970-2979.

Manning AL, Longworth, MS, and Dyson NJ (2010) Loss of pRB causes centromere dysfunction and chromosomal instability. *Genes Dev* **24**:1364-1376.

Martin-Lluesma S, Stucke VM, and Nigg EA (2002) Role of Hec1 in spindle checkpoint signaling and kinetochore recruitment of Mad1/Mad2. *Science* **297**:2267-2270.

Mayr MI, Hummer S, Bormann J, Gruner T, Adio S, Woehlke G, and Mayer TU (2007) The human kinesin Kif18A is a motile microtubule depolymerase essential for chromosome congression. Curr Biol **17**:488-498.

McEwen, BF, Chan GK, Zubrowski B, Savoian MS, Sauer MT, and Yen TJ (2001) CENP-E is essential for reliable bioriented spindle attachment, but chromosome

alignment can be achieved via redundant mechanisms in mammalian cells. *Mol Biol Cell* **12**:2776-2789.

McEwen BF, and Dong YM (2009) Releasing the spindle assembly checkpoint without tension. *J Cell Biol* **184**:355-356.

McEwen BF, Heagle AB, Cassels GO, Buttle KF, and Rieder CL (1997) Kinetochore fiber maturation in PtK1 cells and its implications for the mechanisms of chromosome congression and anaphase onset. *J Cell Biol* **137**:1567-1580.

McIntosh JR, Grishchuk EL, Morphew MK, Efremov AK, Zhudenkov K, Volkov VA, Cheeseman IM, Desai A, Mastronarde DN, and Ataullakhanov FI (2008) Fibrils Connect Microtubule Tips with Kinetochores: A Mechanism to Couple Tubulin Dynamics to Chromosome Motion. *Cell* **135**:322-333.

Mimori-Kiyosue Y, Grigoriev I, Sasaki H, Matsui C, Akhmanova A, Tsukita S, and Vorobjev I (2006) Mammalian CLASPs are required for mitotic spindle organization and kinetochore alignment. *Genes to Cells* **11**:845-857.

Mountain V, Simerly C, Howard L, Ando A, Schatten G, and Compton DA (1999) The kinesin-related protein, HSET, opposes the activity of Eg5 and cross-links microtubules in the mammalian mitotic spindle. *J Cell Biol* **147**:351-366.

Musacchio A, and Hardwick KG (2002) The spindle checkpoint: structural insights into dynamic signalling. *Nature Rev Mol Cell Biol* **3**:731-741.

Musacchio A, and Salmon ED (2007) The spindle-assembly checkpoint in space and time. *Nature Rev Mol Cell Biol* **8**:379-393.

Nicklas RB, and Arana P (1992) Evolution and the Meaning of Metaphase. *J Cell Sci* **102**:681-690.

Pereira AL, Pereira AJ, Maia ARR, Drabek K, Sayas CL, Hergert PJ, Lince-Faria M, Matos I, Duque C, Stepanova T, Rieder CL, Earnshaw WE, Galjart N, and Maiato H. (2006) Mammalian CLASP1 and CLASP2 cooperate to ensure mitotic fidelity by regulating spindle and kinetochore function. *Mol Biol Cell* **17**:4526-4542.

Rieder CL, Cole RW, Khodjakov A, and Sluder G (1995) The Checkpoint Delaying Anaphase in Response to Chromosome Monoorientation Is Mediated by an Inhibitory Signal Produced by Unattached Kinetochores. *J Cell Biol* **130**:941-948.

Rieder CL, and Khodjakov A (2003) Mitosis through the microscope: Advances in seeing inside live dividing cells. *Science* **300**:91-96.

Salmon ED, Cimini D, Cameron LA, and DeLuca JG (2005) Merotelic kinetochores in mammalian tissue cells. Philo Trans Royal Society London **360**:553-568.

Stumpff J, von Dassow G, Wagenbach M, Asbury C, and Wordeman L (2008) The kinesin-8 motor Kif18A suppresses kinetochore movements to control mitotic chromosome alignment. *Dev Cell* **14**:252-262.

Thein KH, Kleylein-Sohn J, Nigg EA, and Gruneberg U (2007). Astrin is required for the maintenance of sister chromatid cohesion and centrosome integrity. *J Cell Biol* **178**:345-354.

Toso A, Winter JR, Garrod AJ, Amaro AC, Meraldi P, McAinsh AD (2009) Kinetochore-generated pushing forces separate centrosomes during bipolar spindle assembly. *J Cell Biol* **184**:365-372.

Varga V, Helenius J, Tanaka K, Hyman AA, Tanaka TU, and Howard J (2006). Yeast kinesin-8 depolymerizes microtubules in a length-dependent manner. *Nature Cell Biol* **8**:957-962.

Wan XH, O'Quinn RP, Pierce HL, Joglekar AP, Gall WE, DeLuca JG, Carroll CW, Liu ST, Yen TJ, McEwen BF, Stukenberg PT, Desai A, Salmon ED (2009) Protein Architecture of the Human Kinetochore Microtubule Attachment Site. *Cell* **137**:672-684.

Welburn JPI, Grishchuk EL, Backer CB, Wilson-Kubalek EM, Yates JR, and Cheeseman IM (2009) The Human Kinetochore Ska1 Complex Facilitates Microtubule Depolymerization-Coupled Motility. *Dev Cell* **16**:374-385.

Yang ZY, Tulu US, Wadsworth P, and Rieder CL (2007) Kinetochore dynein is required for chromosome motion and congression independent of the spindle checkpoint. *Curr Biol* **17**:973-980.

Zhai Y, and Borisy GG (1994) Quantitative determination of the proportion of microtubule polymer present during the mitosis-interphase transition. *J Cell Sci* **107**:881-890.

Zhai Y, Kronebusch PJ, and Borisy GG (1995) Kinetochore microtubule dynamics and the metaphase-anaphase transition. *J Cell Biol* **131**:721-734.

FIGURE LEGENDS

Figure 1. Astrin stabilizes kMT attachments. (A) Examples of D.I.C. and time-lapse fluorescent images of spindles of control and astrin-depleted U2OS cells at metaphase before (Pre-PA) and at the indicated times (s) after activation (Post-PA) of GFP-tubulin fluorescence. Scale bar, 5-μm. (B) Example of normalized fluorescence intensity over time after photoactivating spindles in A. Datapoints represent mean ± s.e.m., n = 11-19 cells. (C) Kinetochore-microtubule half-life (min.) of control, astrin-depleted, Kif2b-depleted, or astrin/kif2b-depleted U2OS cells at prometaphase and metaphase. Bars represent mean ± s.e.m. derived from the exponential decay curve of the photoactivated fluorescence, (r^2>0.99). *$p < 0.05$, t-test, n = 11-19 cells.

Figure 2. Mutually exclusive complexes of Kif2b/CLASP1 and astrin/CLASP1. (A) Representative examples of U2OS cells at prometaphase and metaphase expressing GFP-Kif2b (green) and stained for astrin (purple) and microtubules (red) and DNA (blue). (B) Representative examples of U2OS cells expressing GFP-Kif2b (green, left panels) and stained for astrin (green, right panels), microtubules (red) and DNA (blue). Cells in left panels were treated with monastrol to enrich for mono-oriented chromosomes. Arrows in right panels point at astrin kinetochore localization on mono-oriented chromosomes. Scale bars, 5-μm (C) Mitotic HeLa cell extracts were immunoprecipitated with anti-astrin (top) or anti-Kif2b serum (bottom). Native protein extracts (Load), unbound proteins (Unbound) and immunoprecipitations (IP) were subjected to western blot analysis with the indicated antibody. (D) HeLa cells stably expressing EGFP-CLASP1 (top left, bottom right), EGFP-Astrin (top right), or U2OS cells stably expressing EGFP-Kif2b (bottom

left) were enriched for mitotic cells by nocodazole treatment (top left, bottom left) or metaphase cells by nocodazole treatment followed by MG132 (top right). Native protein extracts (Load), unbound proteins (Unbound) and immunoprecipitations (IP) were subjected to western blot analysis with the indicated antibody. Immunoprecipitations from (top left) were blotted for LL5β, a known interactor of CLASP1 and, as negative control, α-tubulin (bottom right). Protein extracts from HeLa cells, or HeLa cells stably expressing EGFP-CLASP1, were immunoprecipitated with anti-GFP pre-immunization serum (GFP-PI) antibody and analyzed by western blotting with anti-CLASP1 antibody (bottom right).

Figure 3. The Kif2b/CLASP1, astrin/CLASP1 switch. Representative images of control and astrin-depleted U2OS cells at prometaphase and metaphase expressing GFP-Kif2b (green), microtubules (red) and DNA (blue). Astrin depletion with siRNA constructs described here, or elsewhere (Thein et al., 2007) leads to constitutive GFP-Kif2b localization on bi-oriented kinetochores (bottom panel).

Figure 4. Kif2b/CLASP1 generates poleward force at kinetochores. (A) Schematic diagram showing the requirement for the proteins NuMA and HSET (yellow) for the formation of focused poles in the presence of poleward force (black arrows) at kinetochores (red) (left). In the absence of NuMA and HSET, cells exhibit splayed microtubules (green) at the poles (middle). This can be rescued by abolishing kMT interactions (top right) or poleward force generation in the presence of kinetochore-fibers (bottom right). (B) Representative images of control, Nuf-2, Kif2b-, CLASP1-, astrin-, or

Kif18a-depleted U2OS cells stained for microtubules (green) and DNA (blue). Cells were either untreated (left) or injected with inhibitory antibodies against NuMA and HSET. Scale bar, 5-μm.

Figure 5. Kif18a influences kMT attachments through CLASP1/astrin/Kif2b. (A) Representative images from control or Kif18a-depleted U2OS cells with prometaphase or metaphase. Cells express GFP-Kif2b (green) and are stained for astrin (red) and DNA (blue). (B) Kinetochore-microtubule half-life (min.) of control, Kif18a-, or Kif2b/Kif18a-depleted U2OS cells. Bars represent mean ± s.e.m. derived from the exponential decay curve of the photoactivated fluorescence, (r^2>0.99). *p < 0.05, t-test, n = 10-12 cells.

Figure 6. CLAPS1/astrin/Kif2b contribute to chromosome alignment (A) Representative images of control, Kif2b-, Kif18a- or Kif2b/Kif18a-depleted cells expressing CenpB-GFP to mark kinetochores. All cells had bipolar spindles as judged by DIC images (not shown). (B) The position of selected kinetochore pairs (left axis, red and green lines) and the distance between sister kinetochores (right axis, blue) in (A) as a function of time. (C) Deviation from the average position (μm) of kinetochores (right) as well as deviation from the average inter-kinetochore distance (μm) in control, Kif2b-, Kif18a-, or Kif2b/Kif18a-depleted U2OS cells. Bars represent mean ± s.e.m., n = 59-82 kinetochore measurements.

Figure 7. Mitotic requirements for finely regulated kMT dynamics (A) Mitotic index of U2OS cells depleted of various proteins. Bars represent mean ± s.e.m., n > 500 cells, 5

experiments. p < x, t-test. (B) Representative images of control, astrin-, or astrin/Kif2b-depleted U2OS cells at metaphase stained for kinetochores (red, CREST), mad2 (green) and DNA (blue). Arrows point to mad2-positive kinetochore localization on bioriented chromosomes in astrin depleted cells. Scale bar, 5-μm (C) Percent of anaphase control U2OS cells or cells depleted of various proteins that exhibited one or more lagging chromosomes. (D) Example of a U2OS cell at anaphase with a lagging chromosome. Cells express CenpB-GFP (green) to mark kinetochores and are stained for microtubules (red) and DNA (blue). Scale bar, 5-μm (E) Model for the Kif2b/CLASP1 and astrin/CLASP1 switch at kinetochores. Inter-kinetochore distance influences aurora B activity gradient which recruits the Kif2b/CLASP1 to promote kMT turnover and poleward force generation at the kinetochore. Astrin/CLASP1 displaces Kif2b at the prometaphase-to-metaphase transition to stabilize kMT attachments. Other kinetochore proteins such as Kif18a influence kMT attachments and chromosome alignment by modulating components of this switch.

SUPPLEMENTAL FIGURE LEGENDS

Supplementary Figure 1. Astrin is an outer-kinetochore protein. (A) Representative images of U2OS cells at prometaphase, metaphase and anaphase stained for astrin (red), hec1 (green), and DNA (blue). Scale bar, 5-μm. (B) Normalized astrin fluorescence at kinetochores in cells in early and late prometaphase (P), metaphase (M), and anaphase (A). (C) Localization of astrin in untreated cells in prometaphase and metaphase as well as in mitotic cells treated with monastrol, taxol, or nocodazole as indicated. (D) Normalized astrin fluorescence at kinetochores in cells treated with taxol (T), nocodazole (N), monastrol (M), or monastrol plus hesperadin (M+H). (E) Mitotic HeLa cell extracts were immunoprecipitated with anti-CLASP1. Unbound proteins (Unbound) and immunoprecipitations (IP) were subjected to western blot analysis with antibodies against astrin and Kif2b as indicated.

Supplementary Figure 2. RNAi depletions. Total cell lysates from untreated and astrin- (A), Nuf2- (B), Kif2b- (C), CLASP1- and CLASP2- (D), or MCAK-depleted (E) U2OS cells or GFP-Kif2b expressing U2OS cells (A) were immunoblotted with antibodies specific for astrin (A), Hec1 (B), Kif2b (C), CLASPs (D), MCAK (E), GFP (A), Actin (A-C, E), Kif2a (D), and tubulin (E). U2OS cells depleted of Kif18a, Kif2b, or Kif18a and Kif2b stained for Kif18a (green), microtubules (green), and DNA (blue). Scale bar, 5-μm.

Supplementary Figure 3. Astrin does not perturb sister-chromatid cohesion in U2OS cells. (A) Percent of metaphase chromosome spreads from control, Sgo1-depleted

(Salic et al., 2004), and astrin-depleted U2OS cells that exhibited cohesed sister chromatids. (B) Total cell lysates from cells depleted of astrin using the siRNA sequence described here (astrin RNAi #1) and the siRNA sequence described previously (Thein et al., 2007; astrin RNAi #2). (C) Representative metaphase chromosome spreads from control, Sgo1-depleted and astrin-depleted U2OS cells. (D) Representative metaphase chromosome spreads from control and astrin-depleted cells using the siRNA sequence previously described (Thein et al., 2007) after 10 or 20 hours of nocodazole-mediated mitotic arrest as indicated.

Supplementary Figure 4. Specificity of astrin siRNA knockdowns. (A) HeLa cells were either untreated (Control) or transfected with astrin-specific siRNA sequences from this paper (I), Thein et al., 2007 (II), or targeting the 3'UTR of the astrin mRNA (III & IV) and stained for astrin (red), microtubules (green), and DNA (blue). Scale bar, 10-μm. (B) The percentage of mitotic cells (Mitotic Index) those populations was measured in the presence (+GFP-astrin) or absence of expression of exogenous astrin fused to GFP.

Supplmentary Figure 5. Endogenous Kif2b staining. (A) Untreated U2OS cells or cells depleted of Kif2b or astrin as indicated were stained for Kif2b (green), Hec1 (red), and DNA (blue). Scale bar, 5-μm.

Supplementary Figure 6. Astrin kinetochore localization depends on Nuf2 and CLASPs. (A) Normalized astrin-fluorescence intensity at kinetochores in control, astrin-, CLASP1-, and CLASP1/2-depleted U2OS cells. Bars represent mean ± s.e.m., n = 150

cells, 3 experiments. (B) Representative images of control, astrin-, CLASP1-, CLASP1/2-, or Nuf2-depleted U2OS cells stained for astrin (red), microtubules (green), and DNA (blue). Scale bar, 5-μm.

Supplementary Figure 7. Kif18a localization. Representative images of control, Kif18a-, Kif2b-, or astrin-depleted U2OS cells stained for Kif18a (green), microtubules (red), and DNA (blue). Scale bar, 5-μm.

Supplementary Figure 8. Calcium-stable kMTs in Kif2b- and Kif18a-depleted cells. Representative images of control, and Kif2b/Kif18a-depleted U2OS cells that express CenpB-GFP (green) and are stained for microtubules (red), and DNA (blue). Cells with treated with $CaCl_2$ to eliminate unstable microtubules and expose those that are attached to kinetochores. Scale bar, 5-μm.

Supplementary Figure 9. Specificity of kif2b siRNA knockdowns. U2OS cells were either untreated (Control) or transfected with an siRNA sequence targeting the 5'UTR of the Kif2b mRNA (5'RNAi). The percentages of cells showing lagging chromosomes in anaphase (A) or monopolar spindles (B) decreases upon exogenous expression of GFP-tagged Kif2b (GKb) indicating that these mitotic defects are specific to loss of endogenous Kif2b expression.

A

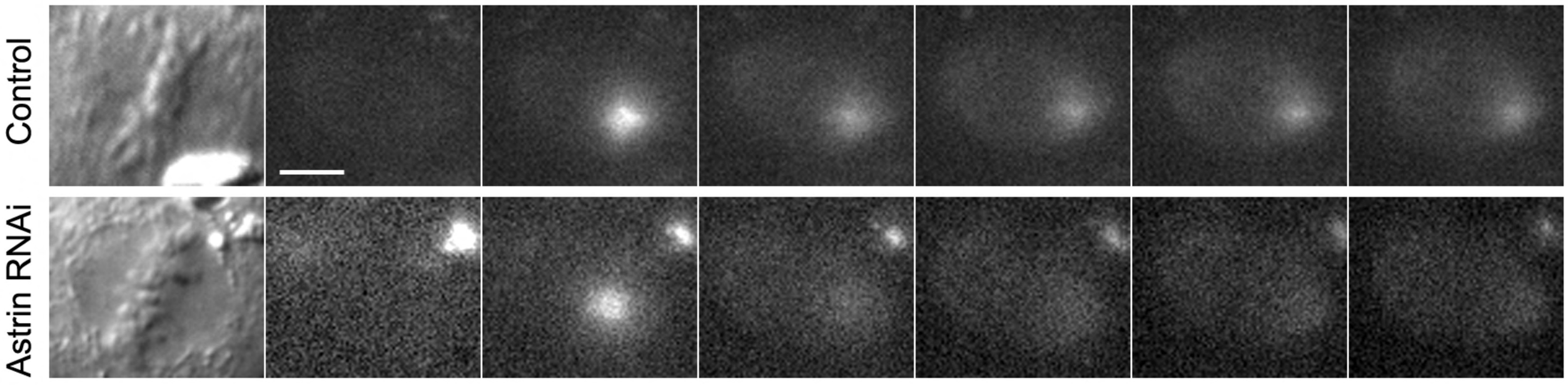
D.I.C.
Pre-PA
Post-PA
60
120
180
240
Control
Astrin RNAi

B

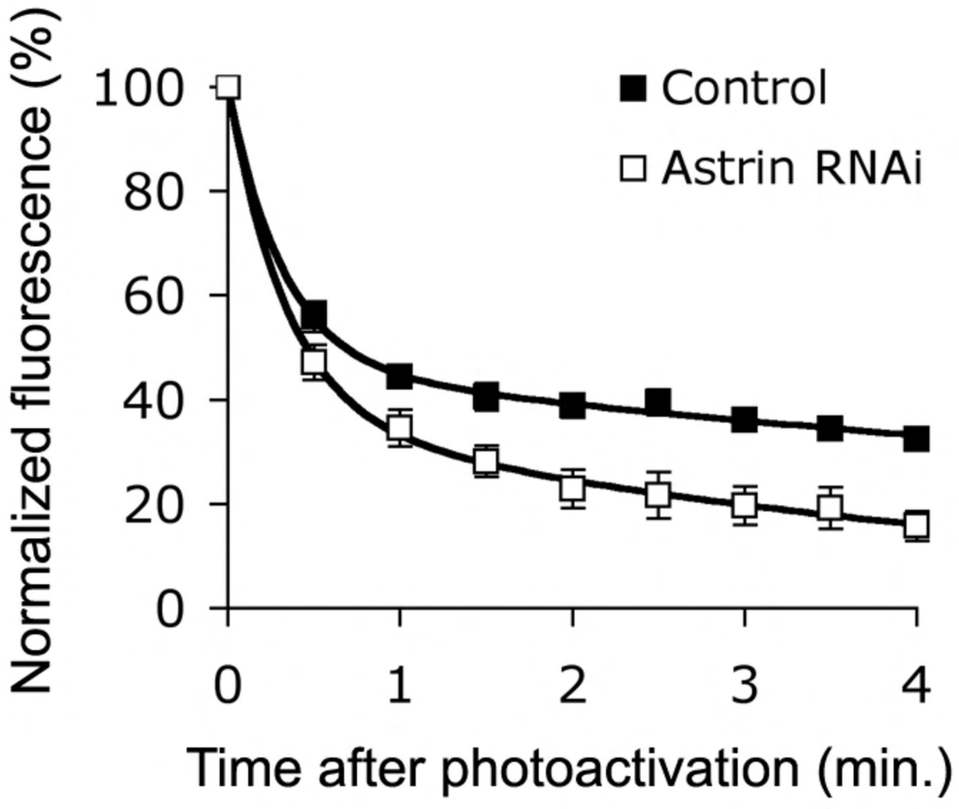
Normalized fluorescence (%)
100
80
60
40
20
0
0
1
2
3
4
Time after photoactivation (min.)
Control
Astrin RNAi

C

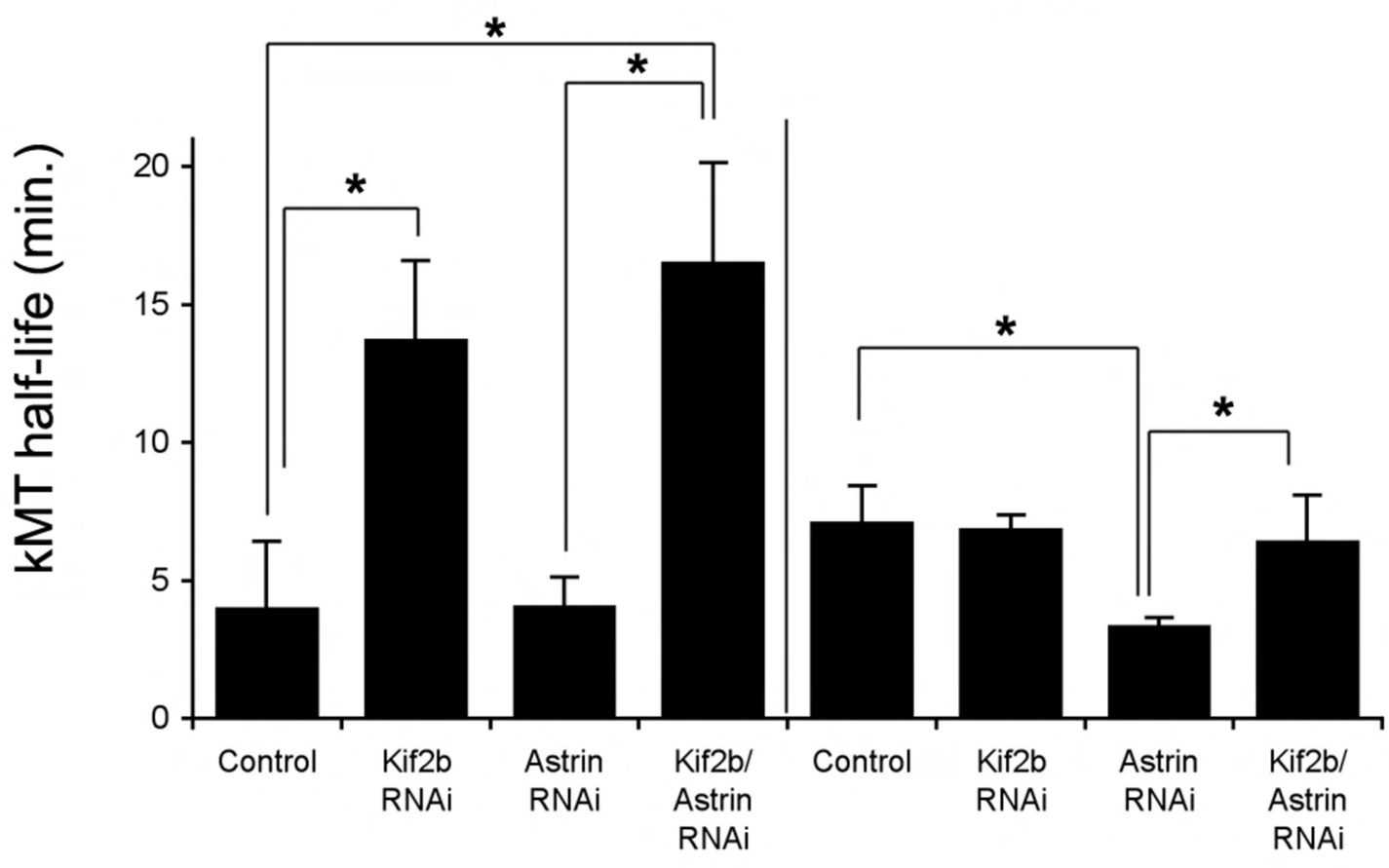
Prometaphase
Metaphase
kMT half-life (min.)
20
15
10
5
0
*
*
*
*
*
Control
Kif2b RNAi
Astrin RNAi
Kif2b/ Astrin RNAi
Control
Kif2b RNAi
Astrin RNAi
Kif2b/ Astrin RNAi

A

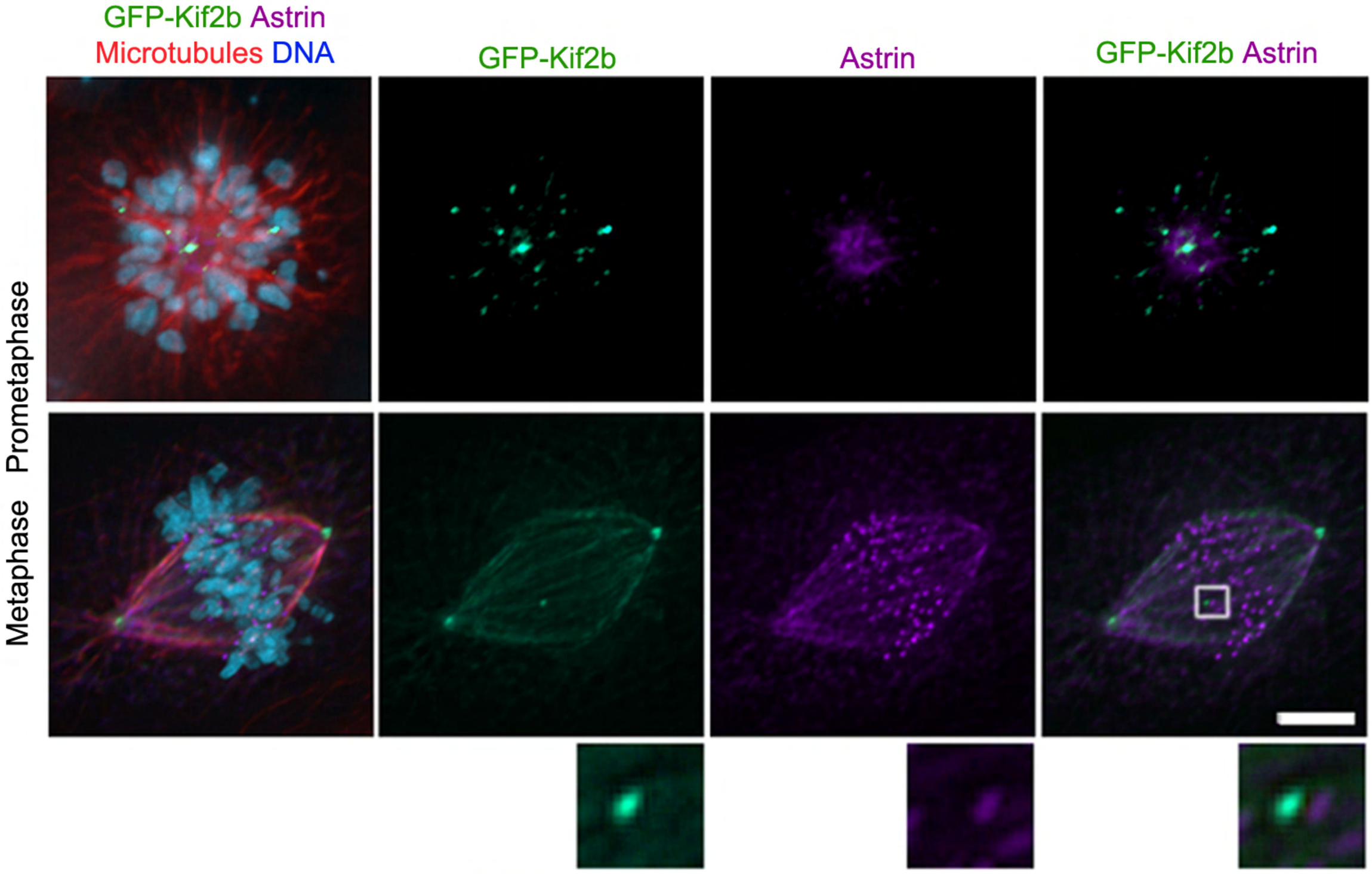
GFP-Kif2b Astrin
Microtubules DNA
GFP-Kif2b
Astrin
GFP-Kif2b Astrin
Prometaphase
Metaphase

B

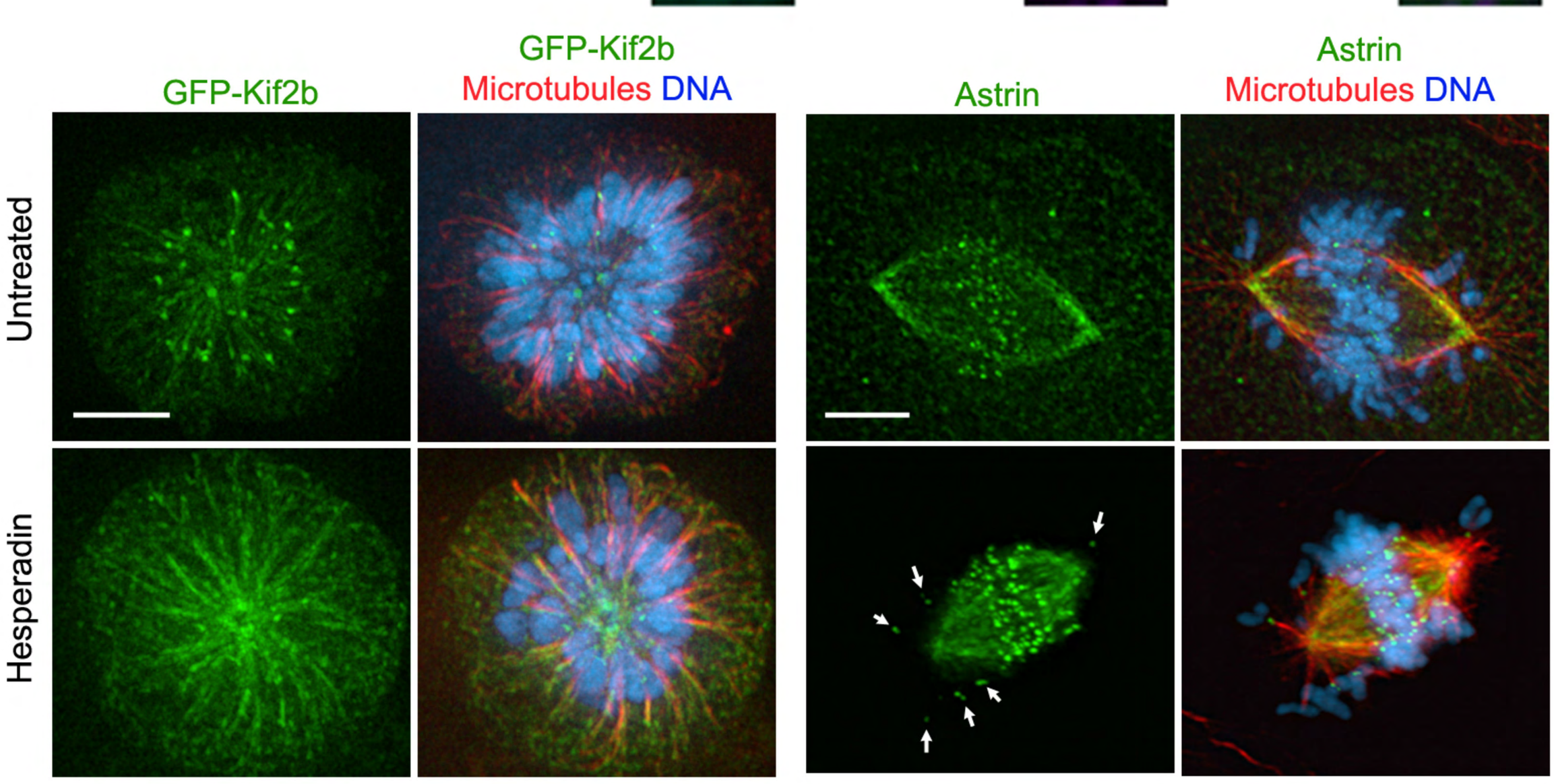
GFP-Kif2b
GFP-Kif2b
Microtubules DNA
Astrin
Astrin
Microtubules DNA
Untreated
Hesperadin

C

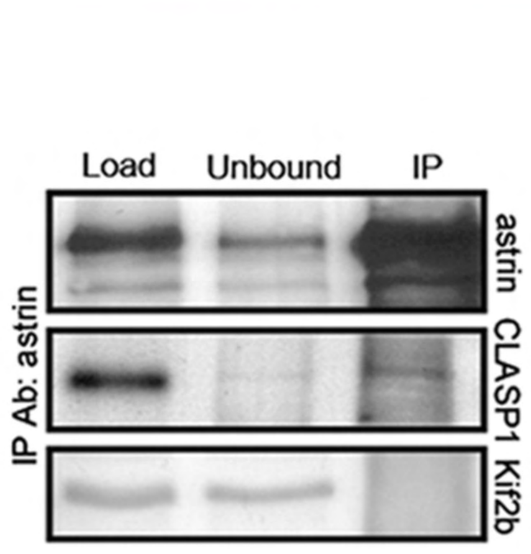
Load
Unbound
IP
IP Ab: astrin
astrin
CLASP1
Kif2b

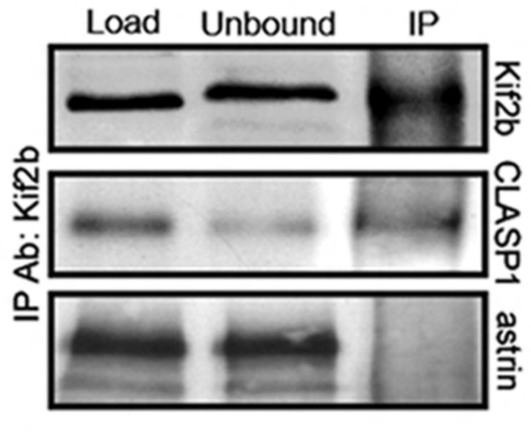
Load
Unbound
IP
IP Ab: Kif2b
Kif2b
CLASP1
astrin

D

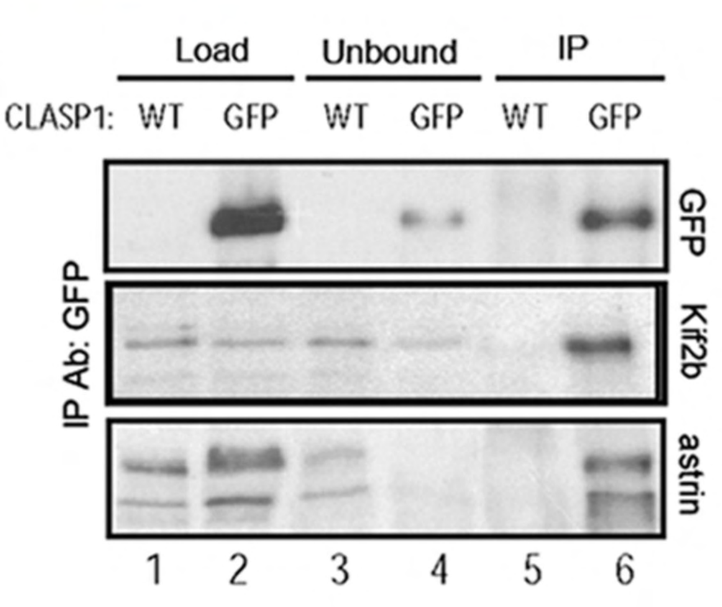
Load
Unbound
IP
CLASP1: WT GFP WT GFP WT GFP
IP Ab: GFP
GFP
Kif2b
astrin
1 2 3 4 5 6

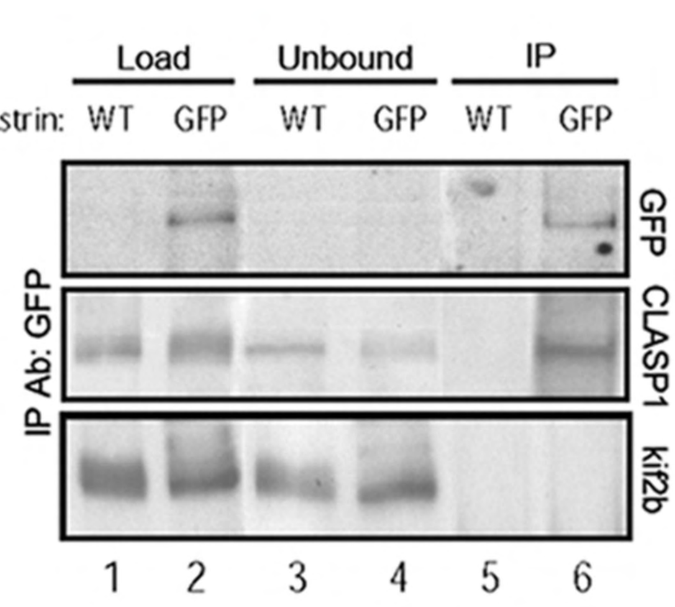
Load
Unbound
IP
Astrin: WT GFP WT GFP WT GFP
IP Ab: GFP
GFP
CLASP1
kif2b
1 2 3 4 5 6

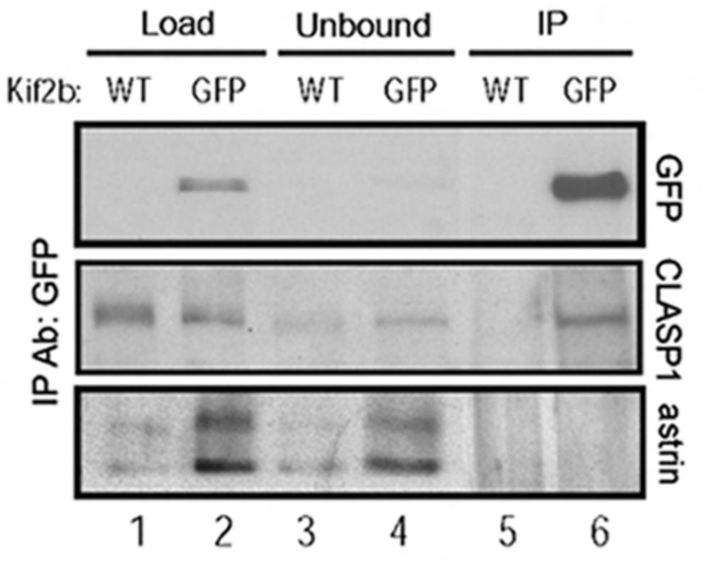
Load
Unbound
IP
Kif2b: WT GFP WT GFP WT GFP
IP Ab: GFP
GFP
CLASP1
astrin
1 2 3 4 5 6

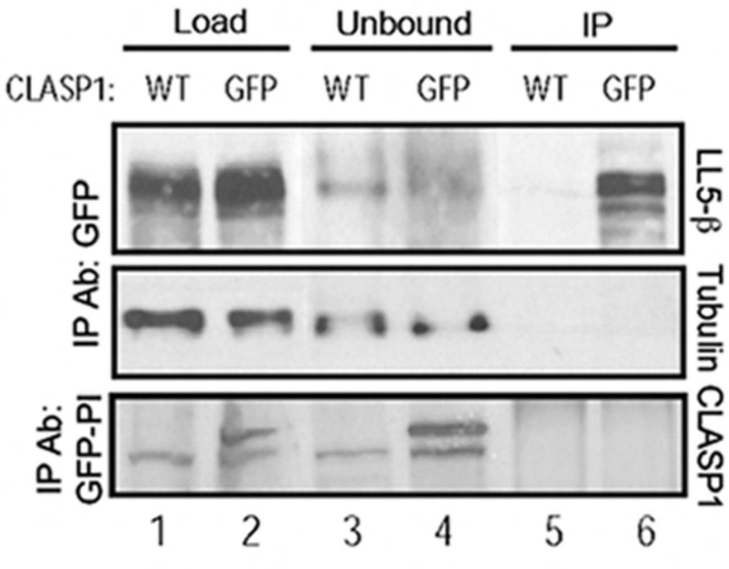
Load
Unbound
IP
CLASP1: WT GFP WT GFP WT GFP
IP Ab: GFP
IP Ab: GFP-PI
LL5-β
Tubulin
CLASP1
1 2 3 4 5 6

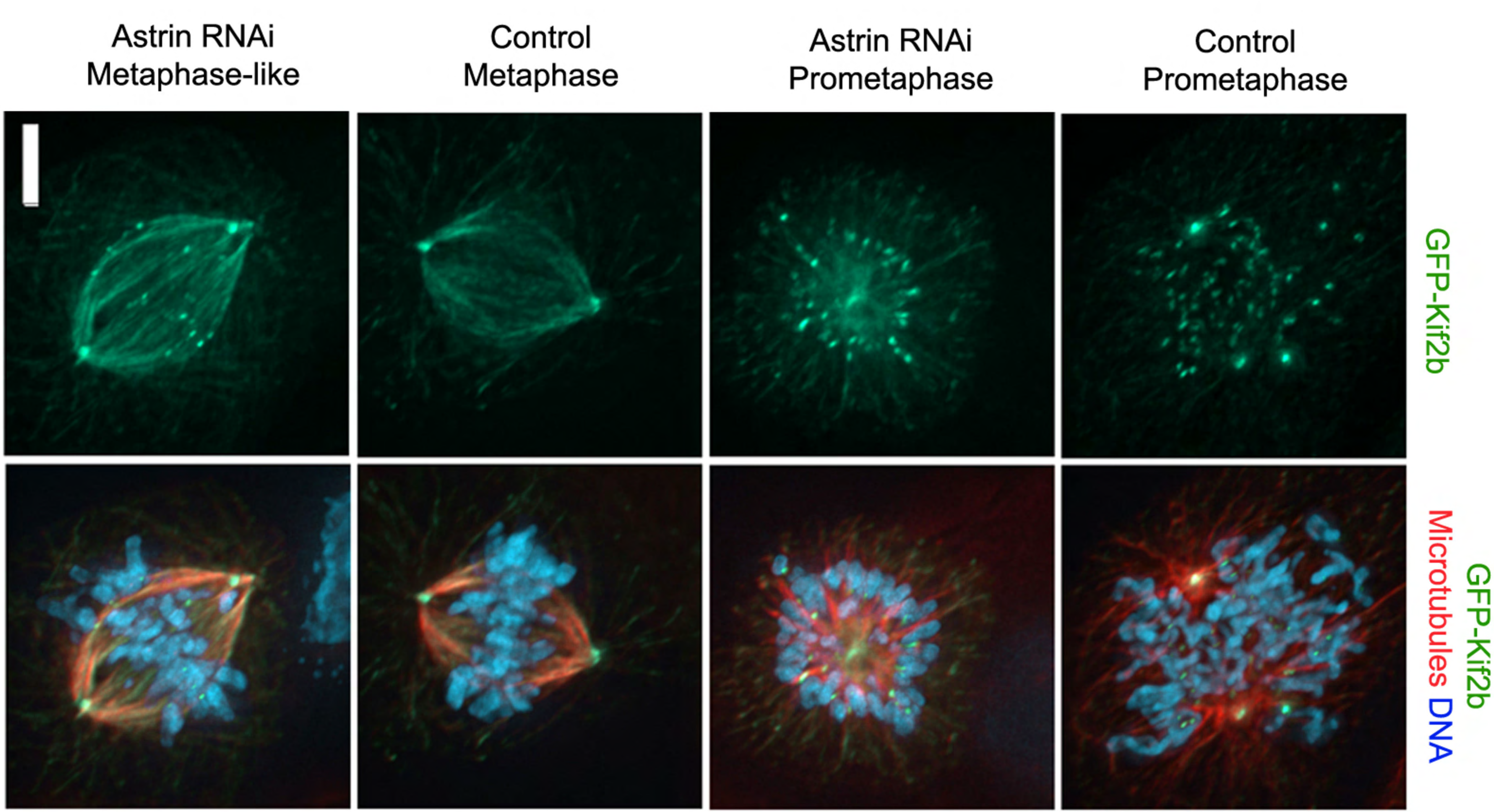
Astrin RNAi
Metaphase-like
Control
Metaphase
Astrin RNAi
Prometaphase
Control
Prometaphase
GFP-Kif2b
GFP-Kif2b
Microtubules DNA

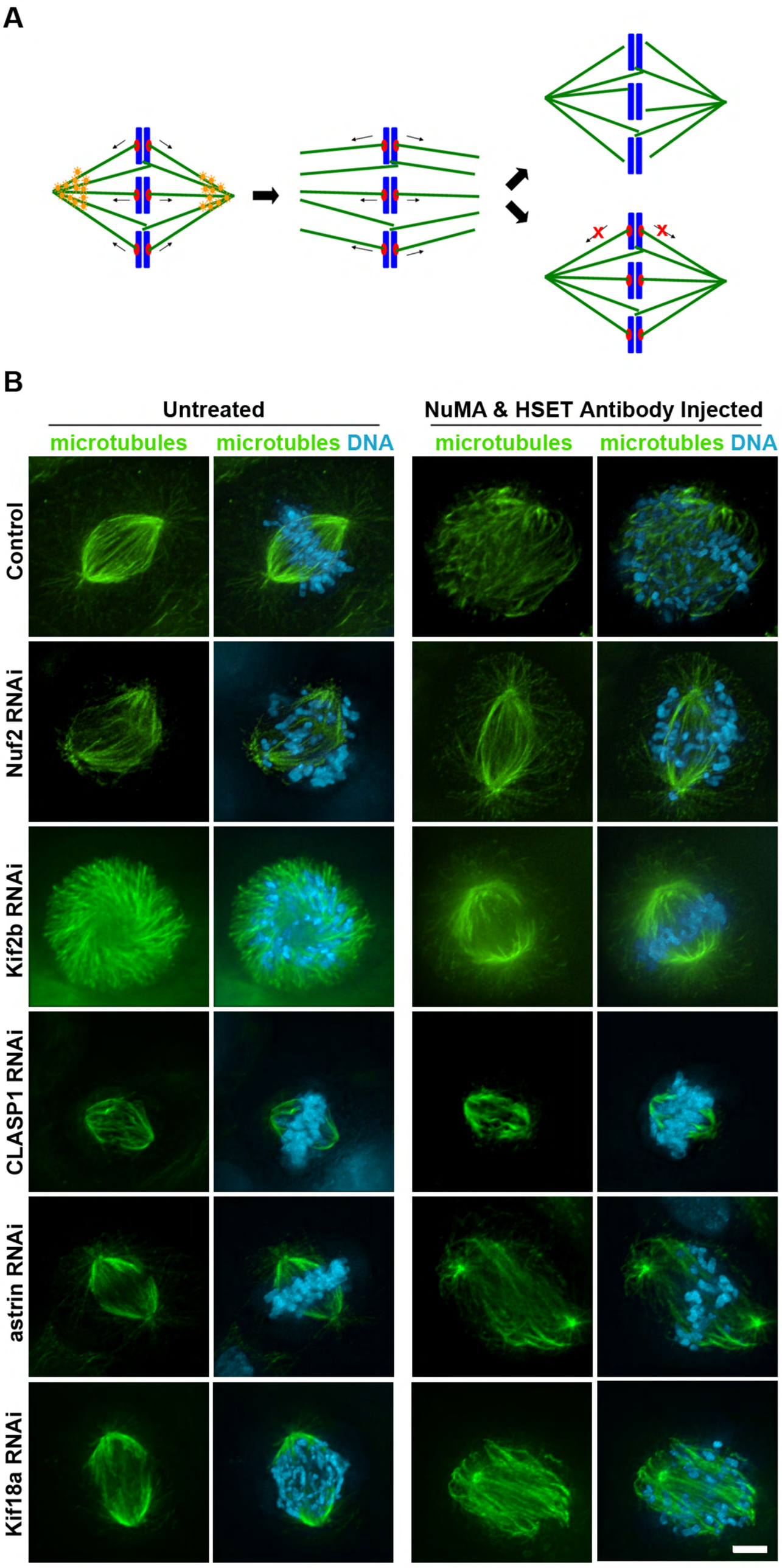
A
B
Untreated
NuMA & HSET Antibody Injected
microtubules
microtubles DNA
microtubules
microtubles DNA
Control
Nuf2 RNAi
Kif2b RNAi
CLASP1 RNAi
astrin RNAi
Kif18a RNAi

A

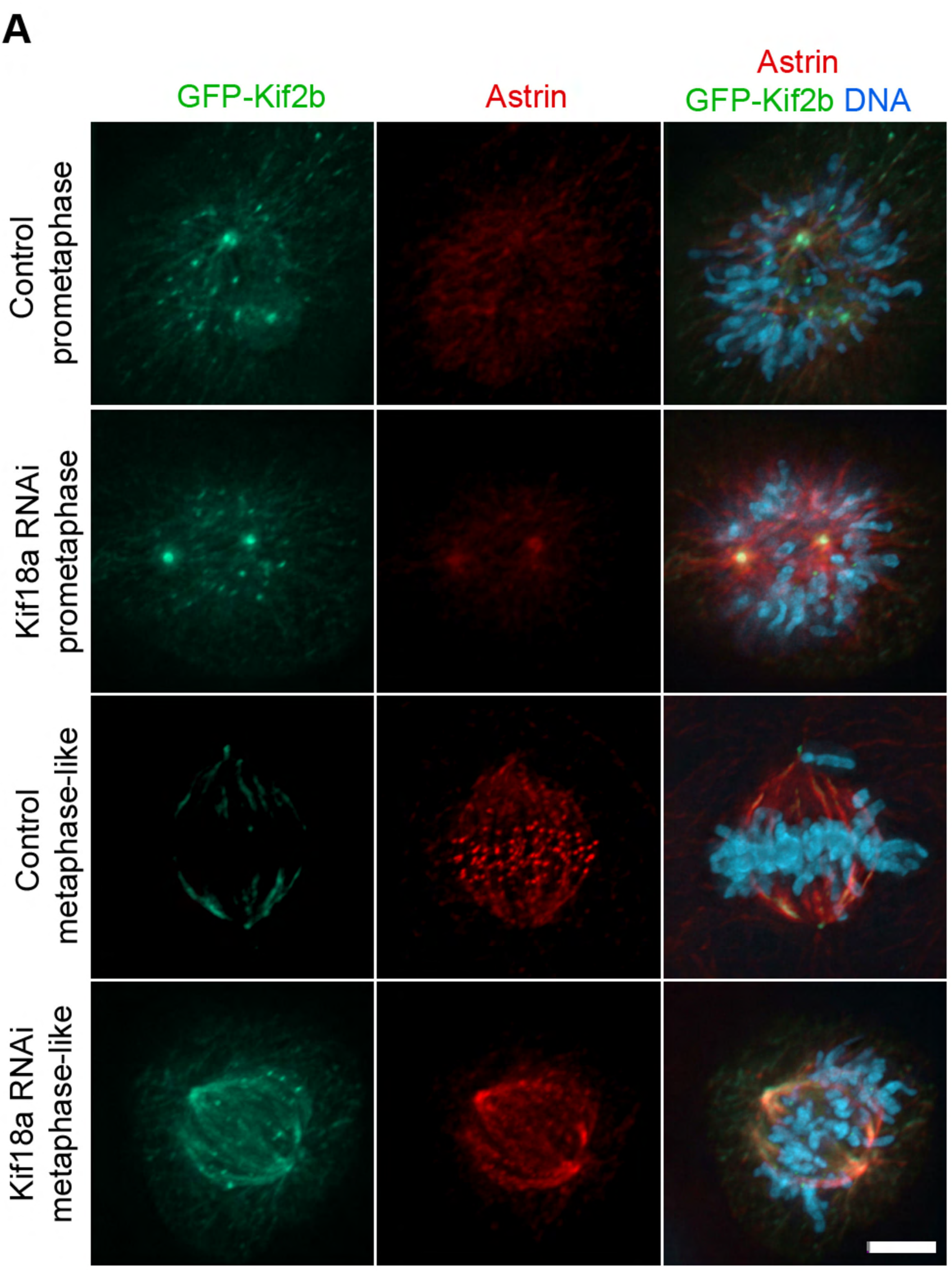
GFP-Kif2b
Astrin
Astrin
GFP-Kif2b DNA
Control prometaphase
Kif18a RNAi prometaphase
Control metaphase-like
Kif18a RNAi metaphase-like

B

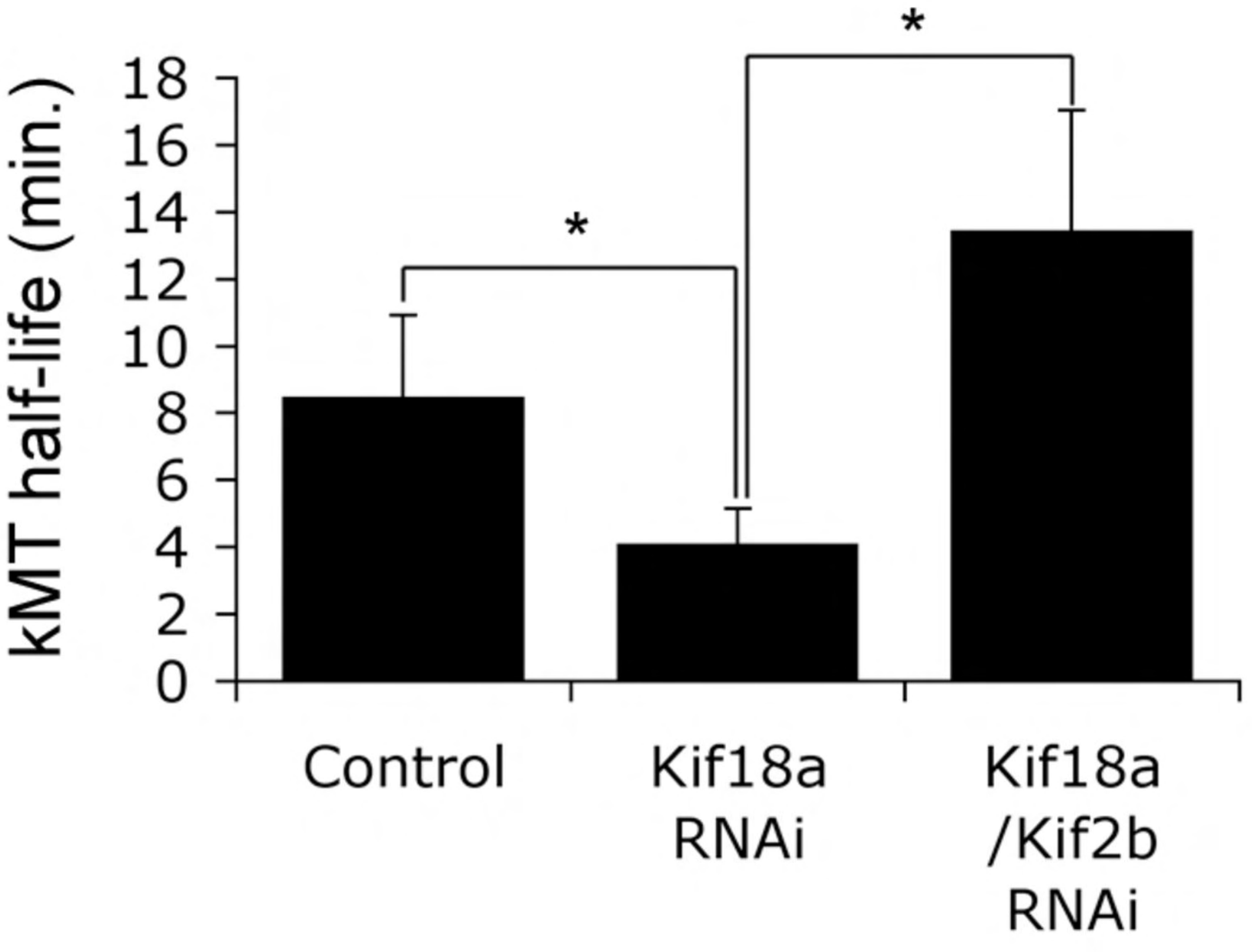
kMT half-life (min.)
0
2
4
6
8
10
12
14
16
18
*
*
Control
Kif18a RNAi
Kif18a /Kif2b RNAi

A

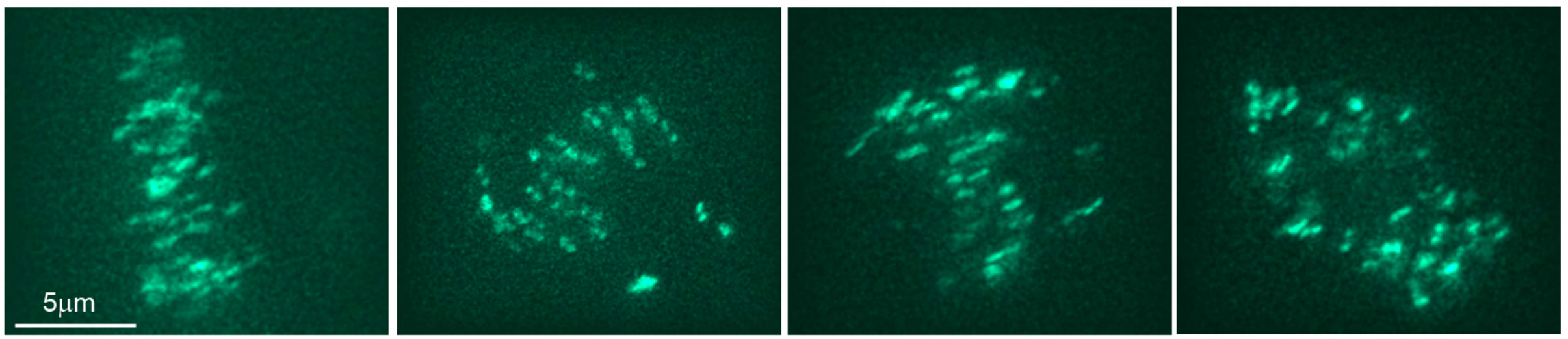
Control
Kif2b RNAi
Kif18a RNAi
Kif2b-Kif18a RNAi
5μm

B

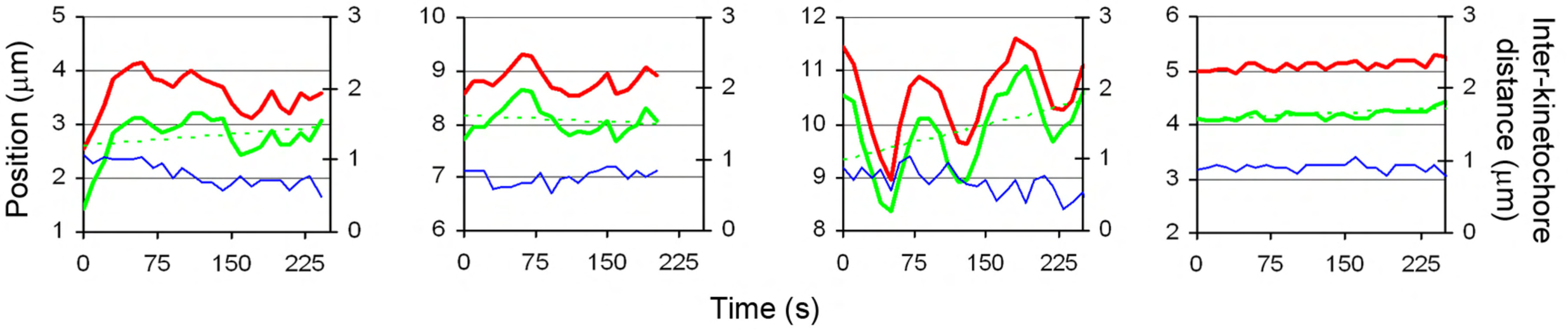
Position (μm)
Inter-kinetochore distance (μm)
Time (s)

C

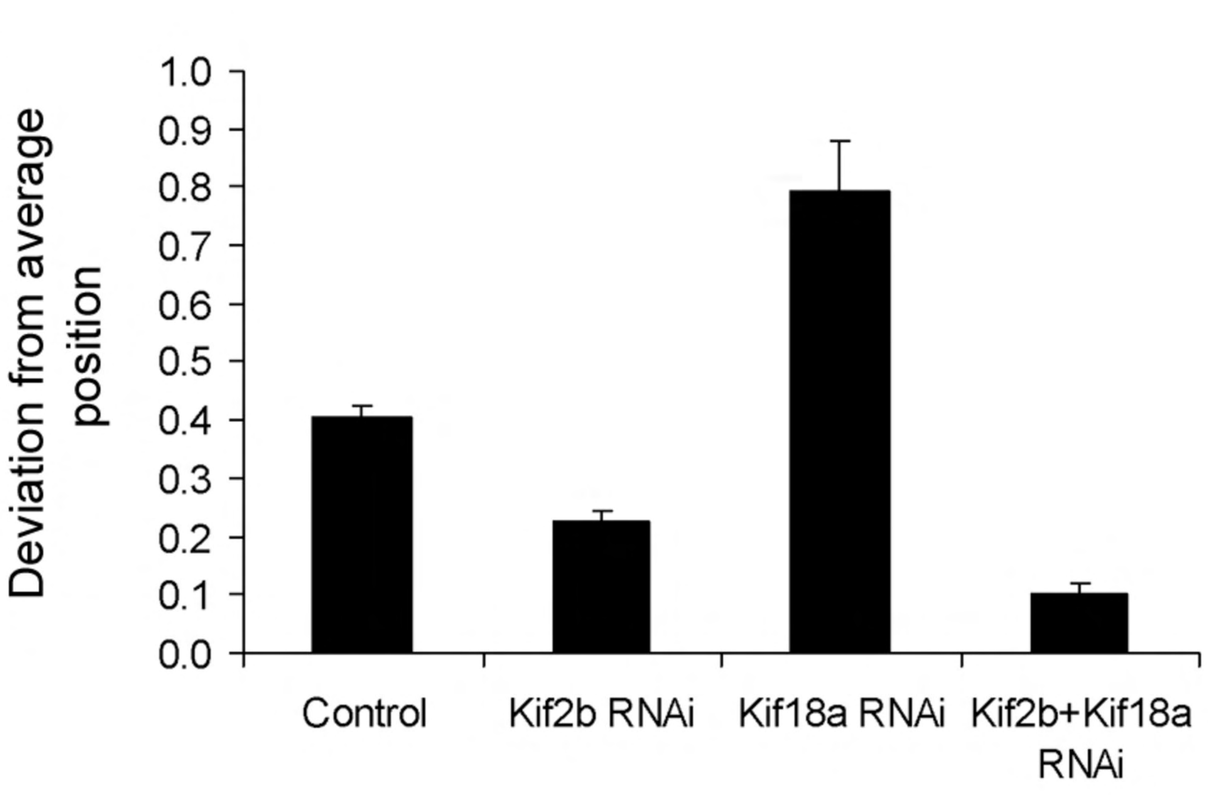
Deviation from average position
Control
Kif2b RNAi
Kif18a RNAi
Kif2b+Kif18a RNAi

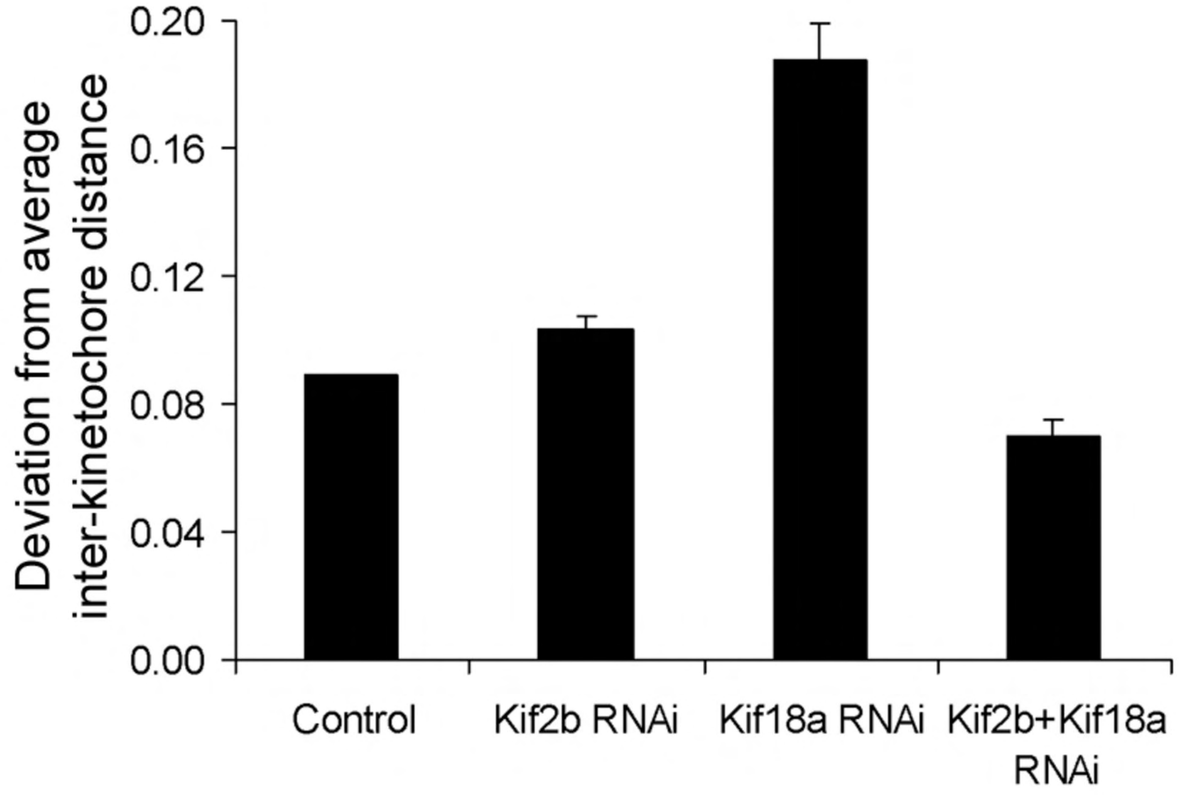
Deviation from average inter-kinetochore distance
Control
Kif2b RNAi
Kif18a RNAi
Kif2b+Kif18a RNAi

A

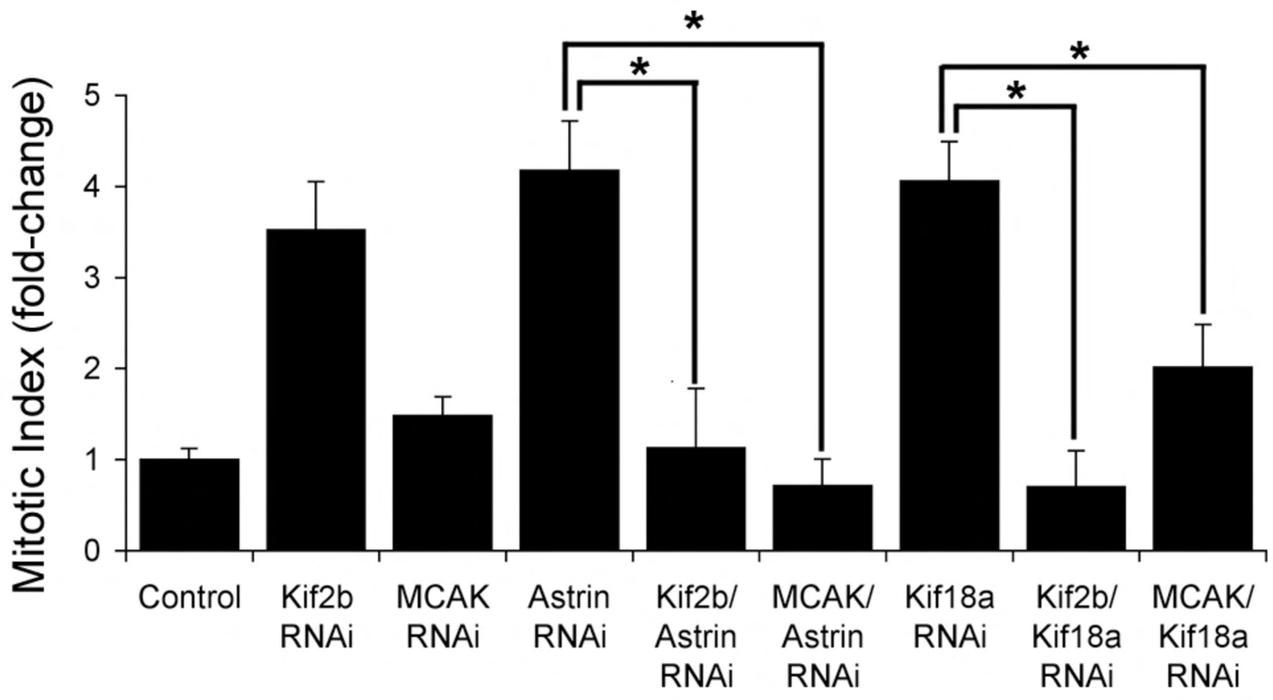
Mitotic Index (fold-change)
0
1
2
3
4
5
*
*
*
*
Control
Kif2b RNAi
MCAK RNAi
Astrin RNAi
Kif2b/ Astrin RNAi
MCAK/ Astrin RNAi
Kif18a RNAi
Kif2b/ Kif18a RNAi
MCAK/ Kif18a RNAi

C

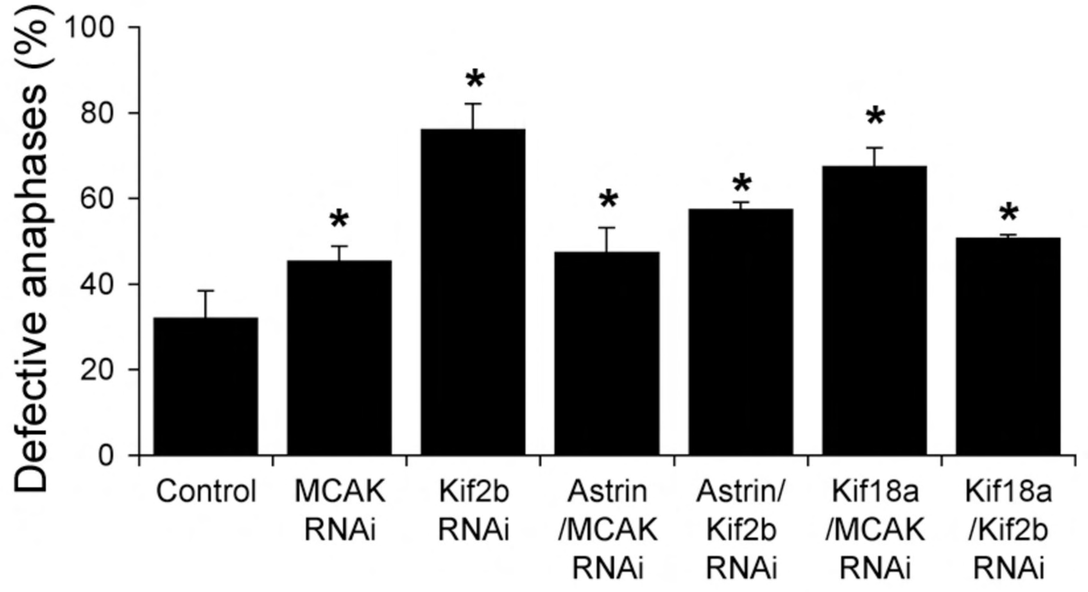
Defective anaphases (%)
0
20
40
60
80
100
*
*
*
*
*
*
Control
MCAK RNAi
Kif2b RNAi
Astrin /MCAK RNAi
Astrin/ Kif2b RNAi
Kif18a /MCAK RNAi
Kif18a /Kif2b RNAi

B

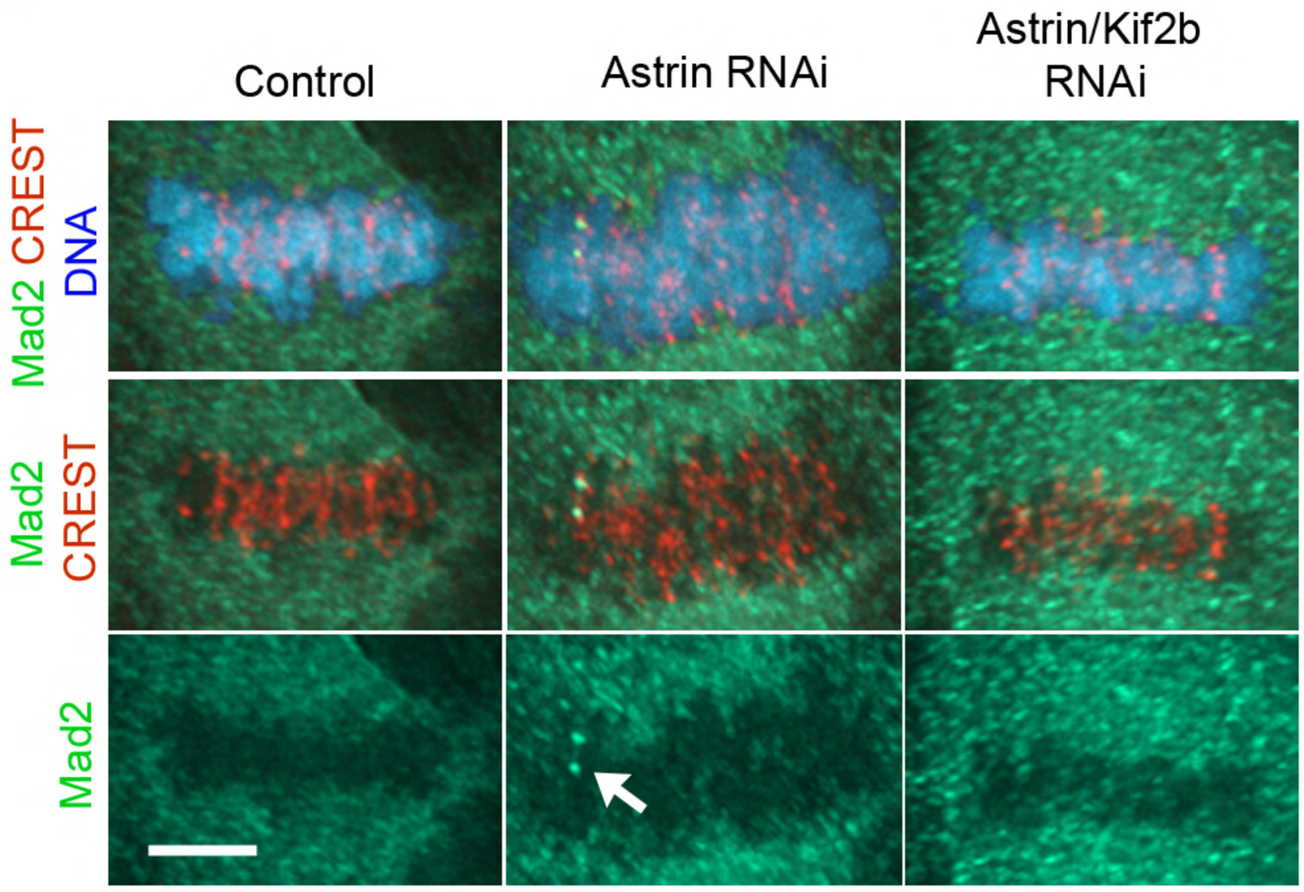
Control
Astrin RNAi
Astrin/Kif2b RNAi
Mad2 CREST DNA
Mad2 CREST
Mad2

D

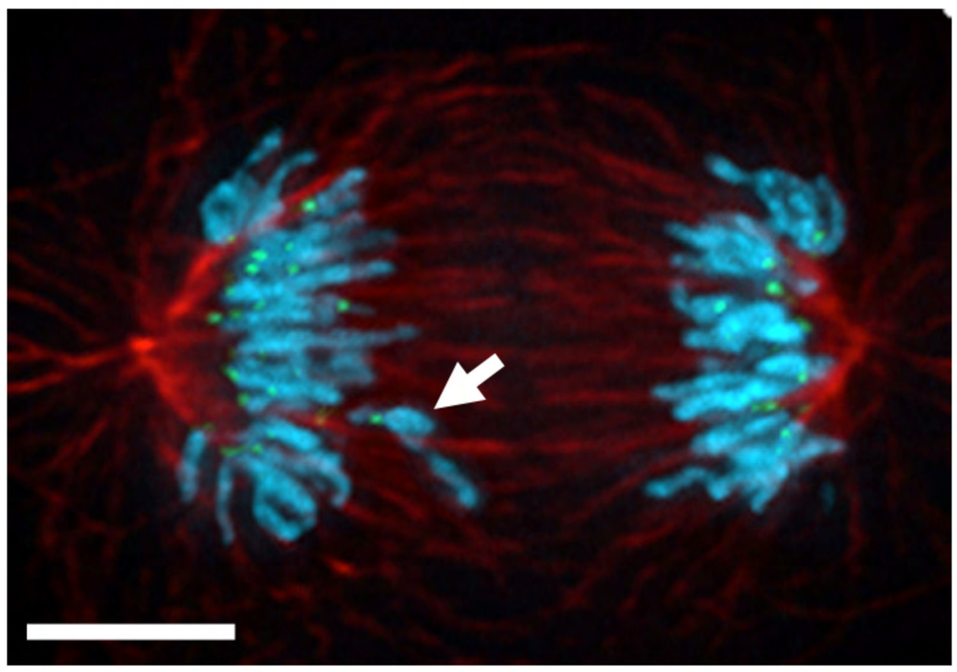
Microtubules
Cenp B
DNA

E

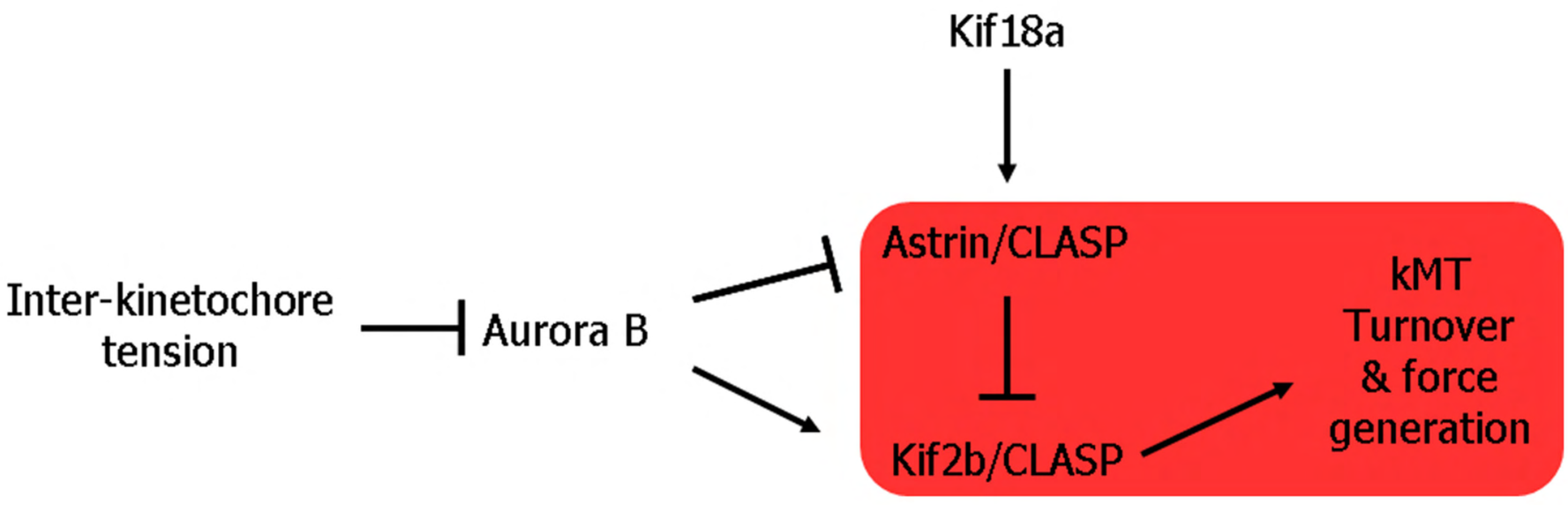
Kif18a
Astrin/CLASP
Inter-kinetochore tension
Aurora B
Kif2b/CLASP
kMT Turnover & force generation